

1 **Understanding aerosol composition in a tropical inter-Andean valley** 2 **impacted by agro-industrial and urban emissions**

3

4 Lady Mateus-Fontecha¹, Angela Vargas-Burbano¹, Rodrigo Jimenez*¹, Nestor Y. Rojas¹, German Rueda-
5 Saa², Dominik van Pinxteren³, Manuela van Pinxteren³, Khandeh Wadinga Fomba³, Hartmut Herrmann³

6

7 ¹ Universidad Nacional de Colombia – Bogota, Department of Chemical and Environmental Engineering, Air Quality Research
8 Group, Bogota, DC 111321, Colombia

9 ² Universidad Nacional de Colombia – Palmira, Department of Engineering and Management, Environmental Prospective,
10 Research Group, Palmira, Valle del Cauca 763533, Colombia

11 ³ Leibniz Institute for Tropospheric Research (TROPOS), Atmospheric Chemistry Department (ACD), Permoserstrasse. 15,
12 04318, Leipzig, Germany.

13 *Correspondence to:* Rodrigo Jimenez (rjimenezp@unal.edu.co)

14 **Abstract.**

15 Agro-industrial areas are frequently affected by various sources of atmospheric pollutants that have a negative impact on public
16 health and ecosystems. However, air quality in these areas is infrequently monitored because of their smaller population
17 compared to large cities, especially in developing countries. The Cauca River Valley (CRV) is an agro-industrial region in
18 Southwest Colombia, where a large fraction of the area is devoted to sugarcane and derivative production. The CRV is also
19 affected by road traffic and industrial emissions. This study aims to elucidate the chemical composition of particulate matter
20 fine mode (PM_{2.5}) and to identify the main pollutant sources before source attribution. A sampling campaign was carried out
21 at a representative site in the CRV region, where daily-averaged mass concentrations of PM_{2.5} and the concentrations of water-
22 soluble ions, trace metals, organic and elemental carbon, and various fractions of organic compounds (carbohydrates, n-
23 alkanes, and polycyclic aromatic hydrocarbons – PAHs) were measured. The mean PM_{2.5} was $14.4 \pm 4.4 \mu\text{g m}^{-3}$, and the most
24 abundant constituent was organic material ($52.7\% \pm 18.4\%$), followed by sulfate ($12.7\% \pm 2.8\%$), and elemental carbon (7.1%
25 $\pm 2.5\%$), which indicates secondary aerosol formation and incomplete combustion. Levoglucosan was present in all samples
26 with a mean concentration of ($113.8 \pm 147.2 \text{ ng m}^{-3}$) revealing biomass burning as a persistent source. Mass closure using the
27 EC tracer method explained 88.4% of PM_{2.5}, whereas the organic tracer method explained 70.9% of PM_{2.5}. We attribute this
28 difference to the lack of information of specific organic tracers for some sources, both primary and secondary. Organic material

29 and inorganic ions were the dominant groups of species (79% of $PM_{2.5}$). OM_{prim} and OM_{sec} from the EC tracer method
30 contribute 24.2% and 28.5% to $PM_{2.5}$. Inorganic ions make 19.0%, EC 7.1%, dust 3.5%, PBW 5.3%, and TEO 0.9% of $PM_{2.5}$.
31 The aerosol was acidic, with a pH of 2.5 ± 0.4 , mainly because of the abundance of organic and sulfur compounds. Diagnostic
32 ratios and tracer concentrations indicate that most $PM_{2.5}$ was emitted locally and had contributions of both pyrogenic and
33 petrogenic sources, that biomass burning was ubiquitous during the sampling period and was the main source of PAH, and
34 that the relatively low $PM_{2.5}$ concentrations and mutagenic potentials are consistent with low-intensity, year-long BB and
35 sugarcane PHB in CRV.

36

37

38 Keywords: agro-industry; pre-harvest burning; $PM_{2.5}$; chemical speciation; principal component analysis; Northern South
39 America

40

41 1. Introduction

42 Urban and suburban locations, with moderate to high population densities, are exposed to air pollutant emissions, including of
43 fine particulate matter (PM) from industry, road traffic, and other anthropogenic activities. Suburban areas may also be
44 impacted by emissions from agricultural activities (Begam et al., 2016). Air quality in areas under these conditions is
45 infrequently monitored, particularly in developing countries, despite the extensive use of highly emitting practices, including
46 intensive use of insecticides and pesticides, fire for land and crop management, and diesel-based mechanization (Aneja et al.,
47 2008, 2009). Agricultural sources emit pollutants, such as volatile organic compounds (VOC), which are precursors of
48 tropospheric ozone (Majra, 2011) and secondary organic aerosols (SOA) (Majra, 2011). Most agricultural activities also emit
49 $PM_{2.5}$ (solid and liquid particles with an aerodynamic diameter smaller than $2.5 \mu m$), which may contain black carbon (BC)
50 and toxic and carcinogenic pollutants, e.g., polycyclic aromatic hydrocarbons (PAH). Other agricultural activities, including
51 mechanized land preparation, sowing and harvesting, consume significant volumes of fossil fuels, particularly diesel, and emit
52 trace gases (including CO_2 , CO, SO_2 , NO_x , NH_3 , VOC) that also generate O_3 and SOA, all of which affect human health and
53 climate (Yadav and Devi, 2019). Furthermore, agricultural operations are a significant source of nitrogen-containing trace
54 gases (NO_2 , NO, NH_3 , N_2O) that are released from fertilizers, livestock waste, and farm machinery into the atmosphere (Sutton
55 et al., 2011). Also, poultry and pig farming are high emitters of sulfur compounds, particularly H_2S .

56

57 The Cauca River Valley (CRV) is an inter-Andean valley in Southwest Colombia with a flat area of $5287 km^2$ (248-km long
58 by 22-km mean width), a mean altitude of 985 m MSL (Figure 1). CRV is bounded by the Colombian Andes Western and
59 Central Cordilleras, and is located at $\sim 120 km$ from the Pacific Ocean. CRV encompasses the cities of Cali, Colombia's third-

60 largest city with 2.2 million inhabitants (hab), Yumbo (129 khab), an important industrial hub, and Palmira (313 khab), an
61 important agro-industry center.

62

63 CRV hosts a highly efficient, resource-intensive sugarcane agro-industry with one of the highest biomass yields (up to 120 ton
64 ha^{-1}) and the highest sugar productivities in the world ($\sim 13 \text{ ton sugar ha}^{-1}$) (Asocaña, 2018, 2019). Sugarcane farming,
65 harvesting, and transport to mills are all mechanized and use diesel as fuel. Besides, all the sugarcane bagasse is used, either
66 to produce heat and electric power (cogeneration) or as feedstock to the local paper industry. Other significant agro-industrial
67 activities in CRV include poultry and livestock production. CRV is the third largest producer of poultry (351,104 ton yr^{-1}), and
68 the first egg producer (4,559 million units per year) in Colombia (Min.Agricultura, 2020). In addition, CRV produces 15.1%
69 of Colombia's pork meat (over 1 million pigs in stock) (Min.Agricultura, 2019) and 1.8% of national beef production (467,782
70 heads in stock) (Min.Agricultura, 2018). Regarding mobile sources, there are nearly 2 million vehicles (1,951,638 vehicles)
71 registered in CRV. These include the standard urban categories along with off-road unregulated farming machinery. The
72 sugarcane agroindustry uses multi-car trailers towed by diesel-powered tractors, with enough annual activity to be considered
73 an independent source (the activity of which is proportional to the sugarcane harvested area and the distance to sugar mills).
74 Overall, CRV mobile sources consumed 772 million L of gasoline and 590 million L of diesel in 2018 (SICOM, 2018).
75 Moreover, the local airport, very close to Palmira, is of the Colombian west hub, which handled 1.3 million passengers in 2019
76 (Aerocivil, 2019). The other main economic line in CRV is the manufacturing industry, located mainly in the seven largest
77 CRV cities: Cali, Tuluá, Cartago, Jamundí, Yumbo, Buga and Palmira.

78

79 For this research, we made a preliminary estimation of the aggregated PM₁₀ emissions in CRV by putting together disparate
80 source data, including from the stationary source emission inventories of CRV's six largest cities (Cali, Tuluá, Cartago,
81 Jamundi, Palmira, Yumbo and Buga), Cali's and other cities, mobile source emission inventories, and an estimation of
82 sugarcane pre-harvest burning (PHB) (Table S4). According to our preliminary estimates, the manufacturing industry is the
83 main PM₁₀ emitter in CRV, with annual emissions of $\sim 11.1 \text{ kton PM}_{10}$. PM₁₀ emissions from mobile sources ($\sim 3.4 \text{ kton PM}_{10}$
84 year^{-1}) and open-field sugarcane pre-harvest burning ($1.7 \text{ kton PM}_{10} \text{ year}^{-1}$) are a factor ~ 3 and ~ 7 smaller, respectively.
85 Nonetheless, it is worth mentioning the following: 1) The available information was insufficient for estimating PM_{2.5}
86 emissions; 2) No emission data were available on Palmira, the city where our measurement site is located; 3) The stationary
87 emission inventory of Yumbo, an industrial hub with the largest industrial activity, is outdated and very likely overestimated,
88 particularly as a significant fraction of coal-fired boilers there have been converted to natural gas. The multiplicity, disparity,
89 and uncertainty of sources are indicative of the complexity of the PM_{2.5} source identification, quantification, and location tasks.

90

91 The determination of the particulate matter (PM) chemical composition instrumental for the apportionment of pollutant
92 sources. Most field measurement-based studies have been conducted in North America, Europe, and Asia (Karagulian et al.,

93 2015). The number of studies in Latin America and the Caribbean (LAC) is much smaller and have focused on the chemical
94 composition of PM₁₀ (Pereira et al., 2019; Vasconcellos et al., 2011), as well as the PM source apportionment in urban areas
95 of Colombia (Ramírez et al., 2018; Vargas et al., 2012), Chile (Jorquera and Barraza, 2012, 2013; Villalobos et al., 2015),
96 Costa Rica (Murillo et al., 2013) and Brazil (de Andrade et al., 2010). The number of studies that involve agro-industrial
97 sources and their impact on suburban areas is smaller. These include the Indo-Gangetic plain (Alvi et al., 2020), the Sao Paulo
98 State in Brazil (Gonçalves et al., 2016; Urban et al., 2016), Ouagadougou in Burkina Faso (Boman et al., 2009), the Anhui
99 Province in China (Li et al., 2014), for which the chemical composition of PM_{2.5} and some of its sources have been identified.
100 Likewise, regions in South America with sugarcane agroindustry, such as Mexico (Mugica-Alvarez et al., 2015; Mugica-
101 Álvarez et al., 2016, 2018) and Brazil (de Andrade et al., 2010; De Assuncao et al., 2014; Lara et al., 2005; Pereira et al.,
102 2017), have also reported on their agro-industry impact on PM_{2.5} levels at nearby population centers. They are very few studies
103 on agricultural air quality agroindustry in Colombia. Most notably, Romero et al., (2013) measured PAHs and metals in PM₁₀.
104 Most of the studies above identified biomass burning and fossil fuel combustion as significant PM sources, and some also
105 identified industrial and fertilizer as relevant.

106

107

108 This research aimed to characterize the chemical composition of PM_{2.5} at a representative location in the CRV, including EC,
109 primary and secondary OC, ions, trace metals, and specific molecular markers, such as PAH, n-alkanes, and carbohydrates, as
110 well as the relationships among these components and with emission sources. Diagnostic ratios were used to identify the most
111 important PM_{2.5} components and as a tool for preliminary pollutant source attribution, including primary and secondary
112 aerosols generated by or associated with sugarcane pre-harvest burning PHB. We believe that in the CRV case, this analysis
113 is needed prior to source apportionment with receptor models for three reasons: 1) This is the first comprehensive investigation
114 of PM composition in the CRV (prior studies included two types of components at most); 2) There are no suitable chemical
115 profiles for some pollutant sources, particularly sugarcane PHB; 3) Our measurements dataset is just barely large enough for
116 profile-free receptor modeling (positive matrix factorization). Our results are particularly relevant for urban communities and
117 atmospheres impacted by large-scale intensive agriculture and industrial emissions, particularly in developing countries,
118 especially in Latin America where PM composition information is still scarce (Liang et al., 2016).

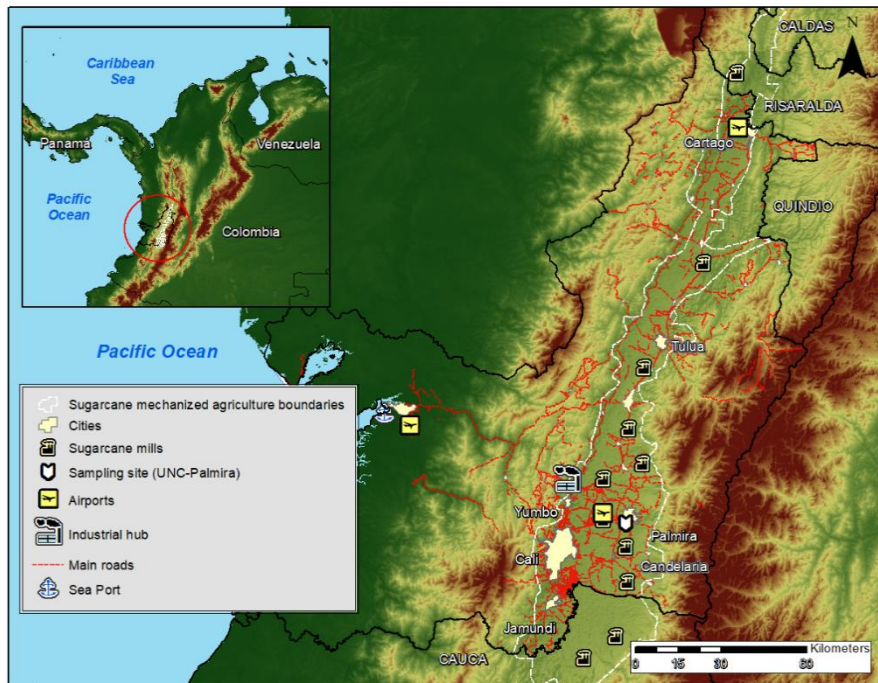
119

120 **2. Methods**

121 **2.1. Description of the sampling site**

122 The sampling site was located on the rooftop of an 8-story administrative building at the Palmira Campus of Universidad
123 Nacional de Colombia (3°30'44.26" N; 76°18'27.40" W, 1065 m altitude), about 27 m above the ground. The campus is located

124 on the western outskirts of Palmira's urban area and is surrounded by short buildings on the east, and extensive sugarcane
 125 plantations, several sugar mills, and other industries elsewhere. Palmira is located at ~27 km northeast of Cali and ~22 km
 126 southeast of Yumbo, an important industrial hub. The Pacific Ocean coastline stretches at ~120 km across the Western
 127 Cordillera, as shown in Figure 1, where operates one of the busiest international trade seaports in Colombia the country (López,
 128 2017). Most of the freight is transported by diesel-powered trucks. Road traffic is also substantial within the CRV, with Bogota
 129 and along the Pan-American highway that connects Colombia with other South American countries (Orozco et al., 2012).



130
 131 Figure 1. Map of the Cauca River Valley (CRV). The inset shows the location of CRV in Colombia and in Northern South
 132 America. The map shows the main cities in CRV, including Palmira (312 thousand inhabitants), our measurement site, Cali,
 133 the largest city in the southwest of Colombia, Yumbo, an industrial hub, and the main highways. Sugar mills, which produce
 134 sugar, bio-ethanol, and electric power are also shown. The dashed-line defined area is CRV's flattest (slope < 5%) bottomland,
 135 where mechanized, intensive sugarcane agriculture takes place. Significant diesel combustion emissions occur along the
 136 Buenaventura highway because it is one of the busiest ports in Colombia.

137

138 The Andes Cordillera splits into three south-to-north diverging mountain ranges (Western, Central, and Eastern Cordilleras)
 139 near the Colombia-Ecuador border (see Figure 1). The Western Cordillera separates the CRV from the Colombian Pacific
 140 Ocean watershed, the rainiest region on Earth (Hernández and Mesa, 2020) The elevated precipitation in this basin (Mesa and

141 Rojo, 2020) is due to the presence of a Walker cell convergence zone at the surface, persistent under neutral and La Niña
142 conditions. This synoptic feature is one of the most important determinants of atmospheric circulation in Colombia, with
143 prevailing east-to-west winds in the lower troposphere along with upper troposphere return winds (Mesa and Rojo, 2020). The
144 Andean Cordilleras are nevertheless effective barriers to the Walker circulation near the CRV surface (Lopez and Howell,
145 1967; Mesa S. and Rojo H., 2020). The elevated humidity in the Pacific Ocean watershed and the closeness of the two Andes
146 branches drive a zonal regional circulation pattern, consisting ~~in~~ of west-to-east anabatic winds over the Pacific slope of the
147 Western Cordillera during the daytime followed by rapid katabatic winds in the late afternoon (Lopez and Howell, 1967).
148 These winds rapidly ventilate the CRV during the late afternoon – early evening period on an almost regular basis. CRV is
149 wide (~22 km) and long (~248 km) enough to develop a valley-mountain wind circulation pattern during the daytime. Winds
150 are very mild during this time period and expected to be highly dispersive, i.e. with high turbulence intensities (Ortiz et al.,
151 2019). The arrival of the katabatic “tide” in the late afternoon wipes the valley-mountain wind pattern out (Lopez and Howell,
152 1967).

153 **2.2. Sampling protocols**

154 The sampling campaign was conducted between July 25th and September 19th, 2018. PM_{2.5} aerosol particles (aerodynamic
155 diameter < 2.5 μm) were collected on Teflon and quartz fiber filters simultaneously for 23 h (from 12:00 local time – LT – to
156 the next day at 11:00 LT), using 2 in-tandem low-volume samplers (ChemComb speciation samplers, R&P). Each sampler
157 used an independent pump set at a flow rate of 14 L min⁻¹. For both types of filters, three lab blank filters without exposure
158 were analyzed. Quartz filters were pre-baked at 600 °C for 8 h before sampling to eliminate contaminant trace hydrocarbons.
159 In total, 45 samples were collected. Prior to and after exposure, the filters were conditioned at constant humidity (36±1.5%
160 relative humidity) and temperature (24 ± 1.2 °C) for 24 h before being weighing on a microbalance (Sartorius, Mettler Toledo)
161 with a 199.99 g capacity and 10 μg resolution. PM_{2.5}-loaded filters were saved at Petri boxes previously prepared to avoid
162 cross-contamination of organic species. The filters were subsequently stored at –20°C until analysis to reduce the volatilization
163 of species such as ammonium nitrate and semi-volatile organic compounds. Blank quartz filters were pre-baked and stored
164 following an identical procedure to exposed filters to collect samples. Blank Teflon filters were treated under the same
165 conditions of storage, transport, and analysis as PM_{2.5}-loaded filters.

166

167 By differential weighing, mass concentrations were determined from the Teflon filters. It’s worth mentioning that during the
168 sampling period, 1888 sugarcane PHB episodes occurred. This register was made by the regional environmental agency (CVC,
169 as per its acronym in Spanish), using information from sugar mills about PHB events. The vast majority of these events were
170 intentional, controlled, size-limited (~6 ha median area), and brief (~25-minute median duration) (Fig S1).

171 2.3. Analytical methods

172 The quartz-fiber filter samples were analyzed for ions, metals, elemental and organic carbon, and speciation of the
173 carbonaceous fraction. The Teflon-membrane filter samples were analyzed for metals.

174

175 Two circular pieces with an 8 mm diameter (100.5 mm²) were punched from each quartz and Teflon filter, following the
176 method described by Wadinga Fomba et al., (2020), and extracted using 1 mL of ultrapure water (18 MΩ) in a shaker at 400
177 rpm for 120 min. The extracts were filtered through 0.45 μm syringe filters (Acrodisc Pall). An aliquot of the solution was
178 analyzed for inorganic (K⁺, Na⁺, NH₄⁺, Mg²⁺, Ca²⁺, Cl⁻, NO₃⁻, SO₄²⁻, NO₂⁻, PO₄³⁻, Br⁻, F⁻) and some organic ions (C₂O₄²⁻,
179 CH₃O₃S⁻, and CHO₂⁻) by ion chromatography (IC690 Metrohm; ICS3000, Dionex). Another aliquot was analyzed for
180 carbohydrates, including levoglucosan, mannosan, and galactosan, as described by Inuma et al. (2009a). Organic and
181 elemental carbon were determined from 90.0 mm² filter pieces following the EUSAAR 2 protocol (Cavalli et al., 2010), with
182 a thermal-optical method using a Sunset Laboratory dual carbonaceous analyzer.

183

184 Seventeen metals, including K, Ca, Ti, V, Cr, Mn, Fe, Ni, Cu, As, Se, Sr, Ba, Pb, Sn, Sb, and Cu, were analyzed from Teflon
185 (22 samples) and quartz (23 samples) filters by total reflection X-Ray Fluorescence Spectroscopy – TXRF (TXRF, PICOFOX
186 S2, Bruker). Si was not determined as this element is part of the quartz filter substrate. Metals were analyzed from three 8-mm
187 circular pieces punched from Teflon filters, which were digested a nitric and chloride acid solution for 180 min at 180 °C.
188 After this, 20-μl aliquots of the digested solution were placed on the surface of polished TXRF quartz substrates along with
189 10 μl of Ga solution, which served as an internal standard. This solution was left to evaporate at 100°C. The samples were
190 measured at two angles with a difference of 90° between them to ensure complete excitation of metals. More details on the
191 analytical technique can be found in Fomba et al. (2013).

192

193 Alkanes and PAHs were determined from two circular filter punches (6 mm diameter, 56.5 mm²), using a Curie-point pyrolyzer
194 (JPS-350, JAI) coupled to a GC-MS system (6890 N GC, 5973inert MSD, Agilent Technologies). The chemical identification
195 and quantification of the C₂₀ to C₃₄ n-alkanes, as well as the following organic species were performed using the following
196 external standards (Campro, Germany): pristane, phytane, fluorene (FLE), phenanthrene (PHEN), anthracene (ANT),
197 fluoranthene (FLT), pyrene (PYR), retene (RET), benzo(b)naphtho(1,2-d)thiophene (BNT(2,1)), cyclopenta(c,d)pyrene
198 (CPY), benz(a)anthracene (BaA), chrysene(+Triphenylene) (CHRY), 2,2-binaphthyl (BNT(2,2)), benzo(b)fluoranthene (BbF),
199 benzo(k)fluoranthene (BkF), benzo(e)pyrene (BeP), benzo(a)pyrene (BaP), indeno (1,2,3-c,d)pyrene (IcdP),
200 dibenz(a,h)anthracene (DahA), and benzo(g,h,i)perylene (BghiP), coronene (COR), 9H-Fluorenone (FLO(9H)), 9,10-
201 Anthracenedione (ANT (9,10)) and 1,2-Benzanthraquinone (BAQ (1,2)). Four deuterated PAHs, (acenaphthene-d10,
202 phenanthrene-d10, chrysene-d12, and perylene-d12), and two deuterated alkanes (tetracosane-d50 and tetratriacontane-d70)

203 were used as internal standards, following the analytical method described by (Neustüss et al., 2000). For each analyzed
 204 compound, the sample concentration was calculated by subtracting the average concentration of three blank filters from the
 205 measured concentration.

206 2.4. Diagnostic ratios and mass closure

207 The main PM_{2.5} components were estimated from the concentrations of EC, OC, water-soluble ions (NO₃⁻, SO₄²⁻, NH₄⁺, and
 208 Na⁺), and tracer metal concentrations (Ca, Ti, Fe, Ni, Cu, Zn, As, Se, Sb, Ba, and Pb) as follows: organic material (OM), EC,
 209 ammonium sulfate ((NH₄)₂SO₄), ammonium nitrate (NH₄NO₃), crustal material (dust), other trace elements oxides (TEOs),
 210 and particle-bounded water (PBW). PM_{2.5} closure is described by Eq 1 (Dabek-Zlotorzynska et al., 2011). We used the
 211 Interagency Monitoring of Protected Visual Environment (IMPROVE) equations (Chow et al., 2015) to quantify the
 212 concentrations of main compounds (Table 1). The aerosol particle bounded water content was estimated from the measured
 213 ionic composition, relative humidity, and temperature, following the aerosol inorganic model (AIM) described by (Clegg et
 214 al., 1998), which is available for running online at <http://www.aim.env.uea.ac.uk/aim/model2/model2a.php>. The
 215 thermodynamic equilibrium of the system H⁺- NH₄⁺ - SO₄²⁻ - NO₃⁻- H₂O is described by AIM.

216

$$217 \text{ PM}_{2.5}(\text{mass closure estimated}) = \text{OM}_{\text{pri}} + \text{OM}_{\text{sec}} + \text{EC} + \text{NH}_4\text{SO}_4 + \text{NH}_4\text{NO}_3 + \text{Dust} + \text{TEO} + \text{SS} + \text{PBW} \quad \text{Eq (1)}$$

218 Table 1. Equations used to estimate the main components of PM_{2.5}

Component	Equation	Reference
OM _{prim}	= f_1 OC _{prim}	(Chow et al., 2015) (Turpin and Lim, 2010)
OM _{sec}	= f_2 OC _{sec}	(El-Zanan et al., 2005)
SO ₄	= SO ₄ ²⁻	(Chow et al., 2015)
NO ₃	= NO ₃ ⁻	(Chow et al., 2015)
Dust	= 1.63Ca + 1.94Ti + 2.42Fe (Assuming CaO, Fe ₂ O ₃ , FeO (in equal amounts) and TiO ₂)	(Chow et al., 2015)
PBW	= k (SO ₄ ²⁻ + NH ₄ ⁺)	(Clegg et al., 1998)
TEO	= 1.47[V] + 1.27[Ni] + 1.25[Cu] + 1.24[Zn] + 1.32[As] + 1.2[Se] + 1.07[Ag] + 1.14[Cd] + 1.2[Sb] + 1.12[Ba] + 1.23[Ce] + 1.08[Pb]	(Snider et al., 2016)

219 f_1 = 1.6. This factor was estimated considering the predominant sources.

220 f_2 = 2.1. This factor was estimated by subtracting the non-carbon component of PM_{2.5} from the measured mass.

221 k = 0.32 was calculated using the Aerosol Inorganic Model.

222

223 The EC tracer method was applied to estimate primary (OC_{prim}) and secondary (OC_{sec}) organic carbon (Lee et al., 2010). This
 224 method utilizes EC as a tracer for primary OC, which implies that OC_{prim} from non-combustion sources is deemed negligible.
 225 Primary and secondary OC can be estimated by defining a suitable primary OC to EC ratio ($[OC/EC]_{prim}$). See Eq (2) and Eq
 226 (3). We estimated the $[OC/EC]_{prim}$ ratio as the slope of a Deming linear fit between EC and OC measurements. The term b
 227 corresponds to the linear fit intercept, which can be interpreted as the emitted OC_{prim} that is not associated with EC emissions.
 228 This method is limited by the following assumptions: 1) $[OC/EC]_{prim}$ is deemed constant, despite the reality that it may change
 229 throughout the day depending on factors such as wind direction and the location of the dominant emission sources. Our 23-h
 230 sampling is expected to smooth this variability source out; 2) It neglects OC_{prim} from non-combustion sources; and 3) It assumes
 231 that OC_{prim} is nonvolatile and nonreactive. Departure from these assumptions implies that the estimation of OC_{prim} and OC_{sec}
 232 might be biased, likely underestimating OC_{sec} .

$$233 \quad \quad \quad OC_{prim} = [OC/EC]_{min} * EC + b \quad \quad \quad \text{Eq (2)}$$

$$234 \quad \quad \quad OC_{sec} = OC - OC_{prim} \quad \quad \quad \text{Eq (3)}$$

236
 237 OC_{prim} was also estimated by using an organic tracer method. A simple linear model was applied to find the proportion of
 238 OC_{prim} from three sources that are significant in the CRV, namely fossil fuel combustion (OC_{FF}), biomass burning (OC_{BB}), and
 239 vegetable detritus (OC_{det}). OC_{FF} , OC_{BB} and OC_{det} was quantified using a linear model from the following tracers: BghiP and
 240 IcdP for fossil fuel; levoglucosan for biomass burning; and the sum of the highest molecular weight alkanes ($C_{27} - C_{33}$) for
 241 vegetable detritus.

242 According to Table 1, OM was estimated from OC using conversion factors f_1 and f_2 (Chow et al., 2015), which are dependent
 243 on the OM oxidation level and the secondary organic aerosol formation and aging during transportation. Turpin and Lim
 244 (2001a) recommended an OM/OC ratio of 1.6 ± 0.2 for urban aerosols, and 2.1 ± 0.2 for non-urban aerosols, values comparable
 245 with those found by Aiken et al. (2008), of 1.71 (1.41 – 2.15), where lower values (1.6 – 1.8) are attributed to ground
 246 measurements in the morning, and higher values (1.8 – 1.9) to aircraft sample measurements. BB aerosols can have even higher
 247 f values (2.2-2.6), due to the presence of organic components with higher molecular weights, e.g., levoglucosan. However,
 248 Andreae (2019) recommends a factor of 1.6 for fresh BB aerosol, which is consistent with Hodshire et al (2019). We believe
 249 that traffic and biomass burning are the dominant OC_{prim} sources at our site. Therefore, we used $f_1 = 1.6$ to estimate OM_{pri} . We
 250 used a factor of 2.1 to estimate OM_{sec} from the OC_{sec} fraction. This factor was chosen based on recommended ratios of 2.1 ± 0.2
 251 for aged aerosols (Schauer, 1998).

252

253 Concentration ratios among distinct species were used to chemically characterize and infer the main sources of fine particle
 254 matter at Palmira. As a preliminary proxy for PM_{2.5} acidity, the cation/anion equivalent ratio and the [NH₄⁺]/[SO₄²⁻] molar
 255 ratio were used. The first one is based on electroneutrality and assumes that H⁺ balances the excess of anions in the solution
 256 considered, and the second one ratio is an indicator of acidity attributable to those two ions, which are usually the most
 257 abundant cation and anion contained in the PM_{2.5}. The cation equivalent to anion equivalent ratio was calculated using Eq (4)
 258 and Eq (5) for each term.

259

260 However, these approaches to inferring the PM_{2.5} acidity can result in challenging interpretations, incomplete and incorrect
 261 results due to an indirect connection to the system's acidity (Pye et al., 2020). Therefore, the E-AIM (Extended Aerosol
 262 Inorganics Model) was used to determine the equilibrium state of a system containing water and the following ions: SO₄²⁻,
 263 NH₄⁺, NO₃⁻, Na⁺ and Cl⁻, with an atmosphere of known temperature and relative humidity, without information on gas-phase
 264 concentrations (NH₃, HNO₃ and SO₂), which were not available in this study. The H⁺ mole fraction concentration from E-AIM
 265 IV (Friese and Ebel, 2010), was used to calculate pH following Eq (6). E-AIM requires that the input data for ionic composition
 266 be balanced on an equivalent basis, which means that the sums of the charges on the cations and anions considered in the
 267 system do balance, accordingly [SO₄²⁻] + [NO₃⁻] + [Cl⁻] = [NH₄⁺] + [Na⁺]. The disadvantage of this approach is that it does
 268 not allow for the partitioning of trace gases into the vapor phase. The model is available to run on the following website:
 269 <http://www.aim.env.uea.ac.uk/aim/model4/model4a.php> (last access: 22 January 2022).

270

$$271 \quad AE = \frac{[SO_4^{2-}]}{48} + \frac{[NO_3^-]}{62} + \frac{[C_2O_4^{2-}]}{44} + \frac{[Cl^-]}{35} + \frac{[PO_4^{3-}]}{31.3} + \frac{[NO_2^-]}{46} + \frac{[Br^-]}{79.9} + \frac{[F^-]}{18.9} + \frac{[CH_3O_3S^-]}{95} + \frac{[CHO_2^-]}{45} \quad \text{Eq (4)}$$

$$272 \quad CE = \frac{[Na^+]}{23} + \frac{[K^+]}{39} + \frac{[NH_4^+]}{18} + \frac{[Mg^{2+}]}{12} + \frac{[Ca^{2+}]}{20} \quad \text{Eq (5)}$$

$$273 \quad pH_x = -\log_{10}(a_{H^+}^x) \quad \text{Eq (6)}$$

274

275 Parent PAH ratios are widely used to identify combustion-derived PAH (Khedidji et al., 2020; Szabó et al., 2015; Tobiszewski
 276 and Namieśnik, 2012), although some of them are photochemically degraded in the atmosphere (Yunker et al., 2002).
 277 Additionally, n-alkanes are employed as markers of fossil fuel or vegetation contributions to PM_{2.5}. Carbon number maximum
 278 concentration (C_{max}), carbon preference index (CPI)_m, and wax n-alkanes percentage (WNA%) were the criteria utilized to
 279 determine the n-alkane origin. Table 2 summarizes the diagnostic ratio equations and the expected dominating source based
 280 on the ratio value.

281

282 Table 2. Diagnostic ratios of organic compounds used to infer the sources of PM_{2.5} in this study.

Diagnostic ratios	Equation	Value	Source	References
BeP/(BeP+BaP)		~0.5 < 0.5	Fresh particles Photolysis	(Tobiszewski and Namieśnik, 2012)
IcdP/(IcdP+BghiP)		<0.2 0.2 - 0.5 >0.5	Petrogenic Petroleum combustion Grass, wood and coal combustion	(Yunker et al., 2002) (Tobiszewski and Namieśnik, 2012)
BaP/BghiP		<0.6 >0.6	Non-traffic emissions Traffic emissions	(Tobiszewski and Namieśnik, 2012) (Szabó et al., 2015)
IcdP/BghiP		>1.25 <0.4	Brown coal* Gasoline	(Ravindra et al., 2008)
LMW/(MMW+HMW)		<1 >1	Pyrogenic Petrogenic	(Tobiszewski and Namieśnik, 2012)
C _{max}		< C ₂₅ C ₂₇ - C ₃₄	Anthropogenic Vegetative detritus	(Lin et al., 2010)
CPI	$CPI = 0.5 * \left[\frac{\sum_{19}^{33} C_i}{\sum_{20}^{32} C_k} + \frac{\sum_{19}^{33} C_i}{\sum_{22}^{34} C_k} \right]$	CPI ~1 CPI > 1	Fossil carbon Biogenic	(Marzi et al., 1993) (Kang et al., 2018)
WNA%	$\sum WNA_{C_n} = [C_n] - \left[\frac{(C_{n+1}) + (C_{n-1})}{2} \right]$ $WNA\% = \frac{\sum WNA_{C_n}}{\sum Total\ n - alkanes}$ $PNA\% = 100 - WNA\%$	WNA ~ 100 PNA ~ 100	Biogenic Anthropogenic	(Lyu et al., 2019)

*Used for residential heating and industrial operation.

283

284

285 As all measured variables were subject to analytical uncertainty and temporal variability, linear fitting parameters were
 286 obtained from Deming regressions as recommended for atmospheric measurements (Wu and Zhen Yu, 2018). The Spearman
 287 coefficient was selected instead of Pearson's as an indicator of statistical correlation between chemical components to reduce
 288 the effect of outliers. Derived ratios and other parameters were considered statistically significant when p-values < 0.05. The
 289 statistical analysis was conducted using R version 4.0.2, 24 including the packages corr (0.4.2), mcr (1.2.1), cluster (2.1.0),
 290 tidyverse (1.3.0), ggplot (3.3.2), psych (2.0.9) and openair (2.7-4).

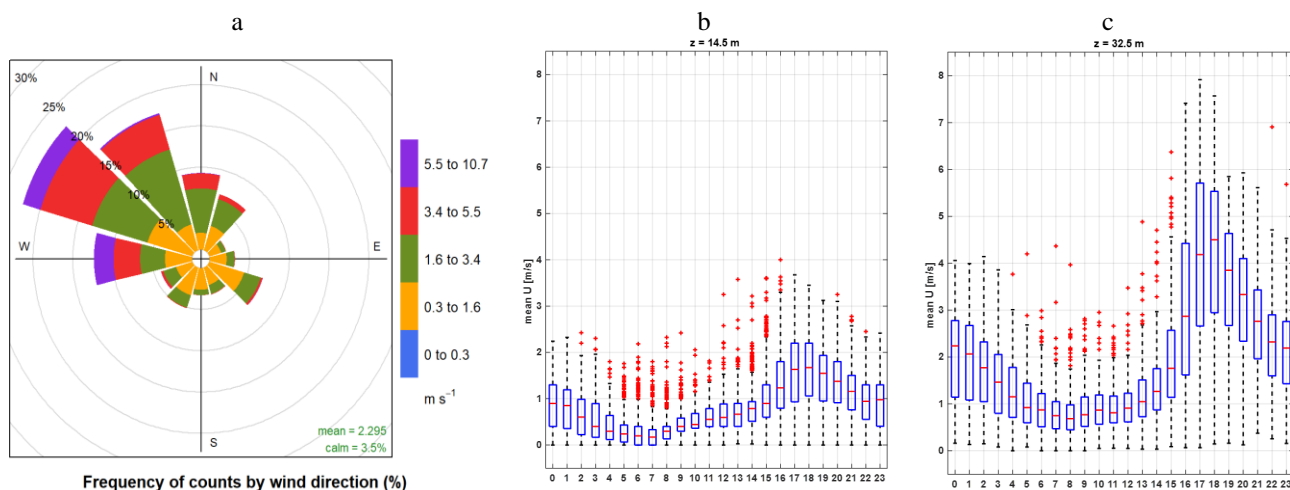
291 3. Results and discussions

292 3.1. Meteorology

293

294 One year prior to the sampling period, we monitored the local meteorology, first at 14.5 m above the ground, a few meters
 295 over the mean canopy level, and then at 32.5 m above the ground during the sampling campaign. The box-and-whisker plot in

296 Fig 2 shows katabatic tide winds of up to ~ 8 m/s at the sampling site elevation, peaking at $\sim 17:00$ LT. Wind speeds were a
 297 factor ~ 2 -3 slower at ground level. The wind runs at the sampling height were typically above ~ 200 km per day (Fig S3)
 298 indicating that the samples had substantially broader spatial coverage of the CRV, much larger than it would have been at
 299 ground level. This also implies that the samples were frequently and significantly influenced by emissions coming from
 300 Yumbo's industrial hub (northwest of Palmira), and also by Palmira and Yumbo urban and highway emissions, as well as
 301 sugarcane PHB and sugarcane mill emissions. The wind rose (Fig 2a) suggests that the influence of urban emissions from Cali,
 302 CRV's largest city by far, was minor. Other meteorological variables are reported in the Supplementary Material (SM) (Fig
 303 S2). Temperature (24.2°C on average) and relative humidity (71.6%) were very likely controlled by solar radiation (350 W m^{-2}
 304 on average). The late-afternoon katabatic tide is fast enough to temporarily reduce temperature. The daily pressure profile
 305 (~ 763 hPa on average) clearly showed the influence of the katabatic tide, with a ~ 3 hPa drop during its arrival in the late
 306 afternoon. Overall, we believe our measurements at the Palmira site are reasonably representative of the regional air quality.



307 Figure 2. Wind pattern in the sampling location: a) predominant wind rose during the sampling period (July - September
 308 2018), b) hourly profile of wind speed at 14.5 m above the ground (August - December 2017), and c) hourly profile of wind
 309 speed in sampling location at 32.5 m over the ground level (December 2017 - September 2018).

310

311 3.2. Bulk $\text{PM}_{2.5}$ concentration and composition

312

313 The daily $\text{PM}_{2.5}$ concentration measured in this study ranged from 6.73 to $24.45 \mu\text{g m}^{-3}$ with a campaign average of $14.38 \pm$
 314 $4.35 \mu\text{g m}^{-3}$ (23 h-average, ± 1 -sigma). Although these concentrations may appear comparatively low, it is worth stressing that
 315 samples were collected at more than 30 m height, with hourly wind speeds frequently above 4 m s^{-1} . However, most days
 316 during this study, $\text{PM}_{2.5}$ concentration exceeded the $5 \mu\text{g m}^{-3}$ annual mean and $15 \mu\text{g m}^{-3}$ 24-h mean guidelines by World Health
 317 Organization, (2021). Nevertheless, the Colombian standards are less demanding, thus observed concentrations comply with
 318 the $37 \mu\text{g m}^{-3}$ 24-h mean (MADS, 2017).

319

320 Previous studies conducted in rural areas of Brazil impacted by open field sugarcane burning reported significantly higher
321 (mean $22.7 \mu\text{g m}^{-3}$; Lara et al., 2005), similar (mean $18 \mu\text{g m}^{-3}$; Souza et al., 2014), and significantly lower $\text{PM}_{2.5}$ concentrations
322 (mean $10.88 \mu\text{g m}^{-3}$; Franzin et al., 2020). Comparable measurements in Mexico during harvest periods showed much higher
323 concentrations, from $29.14 \mu\text{g m}^{-3}$ (Mugica-Alvarez et al., 2015) up to $51.3 \mu\text{g m}^{-3}$ (Mugica-Álvarez et al., 2016). Our $\text{PM}_{2.5}$
324 concentration measurements in the CRV are thus substantially lower than those usually reported in Mexico and Brazil during
325 sugarcane burning periods. Major differences among sugarcane PHB practices in Colombia, Brazil and Mexico must be
326 considered while comparing concentrations. First, $\sim 1/3$ of the sugarcane harvested area is burned before harvest at CRV. This
327 fraction is much larger in Mexico and Brazil (FAO, 2020). Second, sugarcane is harvested year-round in CRV, as opposed to
328 Brazil and Mexico, where harvest is limited to a ~ 6 -month period (known in Spanish as *zafra*, “the harvest”). Third, the size
329 of the individual plots burned in CRV is typically ~ 6 ha (median burned area; Cardozo-Valencia et al., 2019), compared to
330 much larger plots and total areas in Brazil and Mexico (FAO, 2020).

331

332 OC was the most abundant measured $\text{PM}_{2.5}$ component with a mean daily concentration of $3.97 \pm 1.31 \mu\text{g m}^{-3}$, whereas the
333 mean EC concentration was only $0.96 \pm 0.31 \mu\text{g m}^{-3}$. These two components contributed to $29.1 \pm 8.3\%$ and $7.2 \pm 2.3\%$ of the
334 $\text{PM}_{2.5}$ mass, respectively (carbonaceous fractions were thus $4.93 \pm 1.58 \mu\text{g m}^{-3}$, i.e. $36.31 \pm 10.41\%$ of $\text{PM}_{2.5}$).

335

336 The most abundant water-soluble ions found in Palmira’s $\text{PM}_{2.5}$ were SO_4^{2-} , NH_4^+ , and NO_3^- , with average concentrations of
337 $2.15 \pm 1.39 \mu\text{g m}^{-3}$, $0.67 \pm 0.62 \mu\text{g m}^{-3}$, and $0.51 \pm 0.30 \mu\text{g m}^{-3}$, respectively ($12.7 \pm 2.8\%$, $3.7 \pm 1.1\%$ and $2.6 \pm 1.3\%$ of mass
338 concentration, respectively). Other water-soluble ions, such as Na^+ , Ca^+ , and $\text{C}_2\text{O}_4^{2-}$, had mean concentrations of around 0.1
339 $\mu\text{g m}^{-3}$, while those of K^+ , PO_4^{3-} , $\text{CH}_3\text{O}_3\text{S}^-$, Mg^{2+} , and Cl^- had concentrations ranging from 10 - 80 ng m^{-3} (Table 3).

340

341 The predominant elements were Ca ($0.42 \pm 0.33 \mu\text{g m}^{-3}$), K ($0.13 \pm 0.08 \mu\text{g m}^{-3}$), and Fe ($88 \pm 65 \text{ ng m}^{-3}$), followed by Zn (34
342 $\pm 33 \text{ ng m}^{-3}$), Pb ($18 \pm 19 \text{ ng m}^{-3}$), Sn ($52 \pm 37 \text{ ng m}^{-3}$), Ti ($5 \pm 4 \text{ ng m}^{-3}$), Ba ($9 \pm 13 \text{ ng m}^{-3}$), Sr ($2 \pm 5 \text{ ng m}^{-3}$). Mn, Ni, Cr, and
343 Se concentrations were below $2 \pm 1 \text{ ng m}^{-3}$. Trace metals such as Ti, Cr, Mn, K, Ca, Fe, Ni, Cu, Zn Sr, Pb and Se were found
344 in all $\text{PM}_{2.5}$ samples, while V was found only in a few samples. Other trace metals such as As and Sb were detected only at a
345 reduced number of samples with concentrations below 20 ng m^{-3} . Table 3 shows the mean, standard deviation, minimum, and
346 maximum concentration of the carbonaceous fraction, soluble ions, and metals found in the $\text{PM}_{2.5}$ samples collected in the
347 CRV.

348

349 Table 3. Mean, 1 standard deviation, minimum and maximum concentrations of carbonaceous fraction, soluble ions, and
350 metals in samples of $\text{PM}_{2.5}$ collected in Palmira.

Species	# of samples	Mean	SD	Min	Max	Units
PM _{2.5}	22	14.38	4.35	6.73	24.45	μg m ⁻³
OC	45	3.97	1.31	2.31	8.35	
EC	45	0.96	0.31	0.52	2.15	
SO ₄ ⁻²	45	2.15	1.39	0.98	10.27	
NH ₄ ⁺	45	0.67	0.62	0.18	4.29	
NO ₃ ⁻	45	0.51	0.30	0.11	1.45	
Na ⁺	19	0.21	0.16	0.02	0.45	
Ca ⁺² (Water soluble ion)	45	0.14	0.06	0.06	0.28	
C ₂ O ₄ ⁻²	45	0.11	0.06	0.04	0.36	
K ⁺ (Water soluble ion)	45	0.09	0.06	0.02	0.30	
Ca (Trace metal)	42	0.42	0.33	0.01	1.95	
K (Trace metal)	43	0.13	0.08	0.02	0.46	
Formate	13	82	88	0	217	ng m ⁻³
PO ₄ ⁻³	21	66	42	10	148	worldwide
Methansulfonate	45	50	36	13	256	
Cl ⁻	30	20	19	0	75	
Mg ⁺²	45	19	10	2	52	
NO ₂ ⁻	45	3	1	1	6	
Fe	42	88	64	2	293	
Sn	23	52	37	9	137	
Zn	42	34	33	0	153	
Pb	42	18	19	0	84	
Ba	20	9	13	2	72	
Sb	19	8	5	3	22	
Cu	42	6	5	1	22	
Ti	42	5	4	0	17	
As	5	2	4	0	10	
Mn	42	2	1	0	5	
Ni	42	2	1	0	9	
Sr	42	2	5	0	28	
Cr	41	1	1	0	4	
Se	41	1	1	0	6	
V	20	0	1	0	3	

351

352 **3.3. Ions**

353 The SO_4^{2-} and NH_4^+ were the most abundant anion and cation in the $\text{PM}_{2.5}$ samples. The molar ratio between the most abundant
354 cation and anion $[\text{NH}_4^+]/[\text{SO}_4^{2-}]$ was 1.6 ± 0.3 (min: 0.8 and max: 2.3). Acidic conditions in $\text{PM}_{2.5}$ can be inferred, since this
355 ratio was less than two. To assess the acidity of the $\text{PM}_{2.5}$ samples, pH was calculated from of IV E-AIM thermodynamic
356 model, in which the system conformed by H^+ - NH_4^+ - Na^+ - SO_4^{2-} - NO_3^- - Cl^- - H_2O was parametrized to estimate the activity
357 coefficient of these species in aqueous phase equilibrium. As result, the pH of $\text{PM}_{2.5}$ samples collected in the CRV was constant
358 enough, with a mean of 2.5 ± 0.4 . Despite the ions molar ratio do not is centered fact in the pH central concept, the correlation
359 observed between $[\text{NH}_4^+]/[\text{SO}_4^{2-}]$ and pH was strong ($r^2 = 0.96$) as show in Figure S3, which can help to understand the
360 processes of gas - particle partitioning, acid catalytic reactions and metal dissolution that happen in the aerosols observed in
361 CRV (Pye et al., 2020). Fine particles show a bimodal distribution of pH, with a population of particles having a mean pH of
362 1–3, and another population, influenced by dust, sea spray, and potentially biomass burning, having an average pH closer to
363 4–5 (Pye et al., 2020). In this study, just one $\text{PM}_{2.5}$ sample exceed a pH value of 4. Overall, this is an indicator of the abundance
364 of sulfate and organics compounds in samples collected in the CVR.

365

366 The pH affects the partitioning of total nitrate ($\text{NO}_3^- + \text{HNO}_3$) and total ammonium ($\text{NH}_4^+ + \text{NH}_3$) between the gas and
367 particulate phases. Lower pH values favor the partitioning of total nitrate toward the gaseous phase (HNO_3) rather than the
368 particulate phase (NO_3^-). In contrast, the partitioning of total ammonium is favored toward the particulate phase, remaining as
369 NH_4^+ over the aerosol, whereas SO_4^{2-} is a nonvolatile species that remained in the particulate phase. Acidity conditions in the
370 samples collected in this study are consistent with concentrations of SO_4^{2-} , NH_4^+ , and NO_3^- , corresponding to $2.5 \mu\text{g m}^{-3}$, 0.7
371 $\mu\text{g m}^{-3}$, and $0.5 \mu\text{g m}^{-3}$, respectively. Ammoniated sulfate and ammonium nitrate are generally considered the predominant
372 forms of nitrate and sulfate in the inorganic fraction in fine particles. In limited environmental ammonium conditions, ammonia
373 reacts preferentially with H_2SO_4 to form ammonium sulfate ($[\text{NH}_4]_2\text{SO}_4$), letovicite ($[\text{NH}_4]_3\text{H}[\text{SO}_4]_2$) or ammonium bisulfate
374 ($[\text{NH}_4\text{HSO}_4]$) (Lee et al., 2008). Although the correlation coefficient between SO_4^{2-} and NH_4^+ concentrations was high ($R^2 =$
375 0.98), the amount of ammonium contained in the samples was not high enough to neutralize sulfate completely and form
376 $[\text{NH}_4]_2\text{SO}_4$. In environmental with limited concentrations of ammonium, is expected the formation of sulfate salts not
377 completely neutralized, as $[\text{NH}_4]_3\text{H}[\text{SO}_4]_2$ and $[\text{NH}_4\text{HSO}_4]$ (Ianniello et al., 2011). Thus, based on the limited ammonium
378 concentrations found in $\text{PM}_{2.5}$ of CRV, the stoichiometric molar ratio between $[\text{NH}_4^+]/[\text{SO}_4^{2-}]$ of 3:2 for letovicite and 1:1 for
379 ammonium bisulfate, and the results of the E-AIM model, it is possible to indicate that there is a mixture of sulfate salts, such
380 as, ammonium bisulfate, letovicite, and ammonium sulfate, which is going to form progressively, according to ammonia
381 availability. The E-AIM model presents the saturation ratio of each solid species, which usually forms before ammonium
382 bisulfate than letovicite and ammonium sulfate. For a molar ratio of 1.5, the aerosol phase consists almost exclusively of
383 letovicite and to form ammonium sulfate, the ratio should be over 2.0 (Seinfeld and Pandis, 2006).

384

385 The abundance amount of SO_4^{2-} can be attributed to oxidation of SO_2 and SO_3 emitted by from coal fired in power plants and
386 industrial facilities (Wang et al., 2016), the biomass burning activities (Song et al. (2006)) and the emission of H_2S in poultry
387 production animal production system (Casey et al., 2006). The H_2S emission from poultry and pork production is estimated
388 using the factor emission given by animal units (AU) and the time that it stays in the housing, where one AU corresponding to
389 500 Kg of body mass. H_2S emissions from swine and poultry housing trend to be under 5 g $\text{H}_2\text{S AU}^{-1} \text{ d}^{-1}$ Casey et al., (2006),
390 which can reach a 3.5 Ton $\text{H}_2\text{S d}^{-1}$ by poultry and 5 Ton $\text{H}_2\text{S d}^{-1}$ by pork production. Ammonia emissions factors by poultry
391 and livestock vary from 0.09 to 12.9 $\text{AU}^{-1} \text{ d}^{-1}$ which represents 9.05 Ton $\text{NH}_3 \text{ d}^{-1}$ by poultry housing and 12. Ton d^{-1} by pork
392 production.

393

394 In ammonia limited situations, NO_3^- might be bound to cations contained in sea salt and dust particles to form relative
395 nonvolatile salts, as KNO_3 , NaNO_3 and $\text{Ca}(\text{NO}_3)_2$. NO_3^- showed correlation with Na^+ , Ca^{2+} and K^+ ($r^2 = 0.6, 0.2$ and 0.2 ,
396 respectively), indicating possible formation of those salts. The correlation between Na^+ and NO_3^- could be explained by the
397 impact of sea salt aerosol that comes from air mass origin in the Pacific Ocean. However, the amount of Na^+ is not enough to
398 neutralize the total of NO_3^- , while Ca^{2+} showed to be enough amount to neutralize the NO_3^- . The molar ratio observed in $\text{PM}_{2.5}$
399 samples of CRV for $[\text{NO}_3^-]/[\text{Ca}^{2+}]$ was 2.6 ± 1.4 , $[\text{NO}_3^-]/[\text{Na}^+]$ was 1.7 ± 1.3 , and $[\text{NO}_3^-]/[\text{K}^+]$ was 5.0 ± 3.2 , overcoming the
400 stoichiometric molar ratio required to form $\text{Ca}(\text{NO}_3)_2$, NaNO_3 , and KNO_3 .

401

402 Methanesulfonate is produced predominantly by aqueous oxidation of dimethyl sulfide (DMS), one of the most abundant
403 biogenic sulfur compounds in the troposphere. The oxidation of DMS is an important source of non-sea salt sulfate aerosol in
404 marine and oceanic regions (Tang et al., 2019). Methanesulfonate is an organosulfur (OS) compound that can potentially
405 impact the hygroscopicity and surface tension of particles and are useful tracers for secondary aerosol formation (SOA)
406 (Sorooshian et al., 2015). This ion is one of the most easily measured OS species and its concentration can be used as a way
407 of estimating the contribution of biogenic emissions on total sulfate levels. In addition to the oceanic source, methanesulfonate
408 also has terrestrial sources, such as wetlands, freshwater lakes, alfalfa, ruminants, biomass burning, urban and agriculture
409 emissions (Gondwe, 2004; Sorooshian et al., 2015). The [methanesulfonate]/ $[\text{SO}_4^{2-}]$ ratio can be used to infer the origin of its
410 compound and distinguish the impact of fires in the aerosols. In this study the [methanesulfonate]/ $[\text{SO}_4^{2-}]$ ratio was 0.02 ± 0.06
411 (min: 0.012 – max: 0.03), suggesting a minor impact of biogenic sulfur compared to the total inorganic sulfate concentration.
412 However, the correlation between these two ions was very strong ($r^2 = 0.88$). This can be indicative of the existence of OS
413 compounds, not included in this study, as part of the total sulfate levels. According to the average [methanesulfonate]/ $[\text{SO}_4^{2-}]$
414 ratios presented by Sorooshian et al., (2015), coastal regions exhibit higher values (0.06 to 0.09) than inland regions (0.02-
415 0.04). It is then possible to suppose that high methanesulfonate concentrations in the CRV were derived from continental
416 sources. This is supported by the non-existent correlation between Na^+ and methanesulfonate, and the moderate correlation
417 between $\text{C}_2\text{O}_4^{2-}$ and methanesulfonate ($r^2 = 0.66$). Even though the air mass from the Pacific Ocean has an impact on winds

418 that ventilate the CRV in the late afternoon, the western mountain range may act as a barrier for an important fraction of sea
419 salt aerosol.

420

421 The measured average ratio of $[\text{SO}_4^{2-}]/[\text{NO}_3^-] = 4.5 \pm 2.9$. This ratio is higher than the one obtained by Souza et al. (2014) at
422 Piracicaba (3.6 ± 1.0) and Sao Paulo (1.8 ± 1.0), Brazil. The strong correlations between SO_4^{2-} and NH_4^+ ($r^2 = 0.84$), SO_4^{2-} and
423 methanesulfonate ($\text{CH}_3\text{O}_3\text{S}^-$) ($r^2 = 0.88$), and SO_4^{2-} and oxalate dianion ($\text{C}_2\text{O}_4^{2-}$) ($r^2 = 0.71$) allow us to infer that inorganic
424 secondary aerosol formation is a significant $\text{PM}_{2.5}$ source in the CRV. In addition, the presence of potassium cation (K^+) in
425 submicron particles is recognized as a biomass burning tracer (Andreae, 1983; Ryu et al., 2004). K^+ showed a moderate
426 correlation with nitrite anion (NO_2^-) ($r^2 = 0.44$) and $\text{C}_2\text{O}_4^{2-}$ ($r^2 = 0.43$) in the CRV, which suggests that biomass burning
427 influences secondary aerosol formation. Mg^{2+} and Ca^{2+} ions, usually considered crustal metals, exhibited a moderate
428 correlation of $r^2 = 0.59$ (Li et al., 2013). Also, Mg^{2+} and $\text{C}_2\text{O}_4^{2-}$ moderate correlation ($r^2 = 0.26$) points to a link between crustal
429 species and secondary aerosols. Such an association could be plausibly explained by soil erosion induced by pyro-convection
430 during sugarcane pre-harvest burning (Wagner et al., 2018). Our study full species correlation matrix is shown in Fig 4S.

431

432 3.4. Metals

433

434 The measured total $\text{PM}_{2.5}$ trace metal concentration was $706 \pm 462 \text{ ng m}^{-3}$ (101.3 ng m^{-3} to 2638 ng m^{-3}). Trace metals can
435 originate from non-exhaust and exhaust emissions. Non-exhaust emissions come from brake and tire wear, road surface
436 abrasion, wear/corrosion of other vehicle components, and the resuspension of road surface dust (Pant and Harrison, 2013).
437 Metals in exhaust emissions are related to fuel, lubricant combustion, catalytic converters, and engine corrosion. As shown by
438 Kundu and Stone (2014), many of these sources share some metals in their chemical composition profile, thus an unambiguous
439 specific source attribution is non-trivial. In this study, we found a significant correlation among Fe, Mn and Ti ($r^2 \approx 0.72$),
440 which is typically associated with a high abundance of crustal material (Fomba et al., 2018), indicating that soil dust is a
441 significant source in the CRV. Also, tire and brake wear tracer metals, including Zn and Cu, showed weaker but still significant
442 correlations among them ($r^2 \approx 0.32$). Ca concentrations were quite high ($405 \pm 334 \text{ ng m}^{-3}$ (1.6 ng m^{-3} to 1952 ng m^{-3}). These
443 levels can be attributed to dust generation by agricultural practices, particularly land planning, liming and tilling, PHB pyro-
444 convection-induced soil erosion, and traffic-induced soil resuspension on unpaved rural roads. One of the very few previous
445 investigations into on PM composition in the CRV (Criollo and Daza, 2011) analyzed trace metals in PM_{10} at 4 CRV locations,
446 including Palmira. They found significant enrichment of Fe and K metals at locations exposed to PHB. It must be kept in mind
447 that PM_{10} samples included coarse mode aerosols, of which dust might have been a significant fraction. Also, environmental
448 regulations have been successful in steadily reducing the sugarcane burned area in the CRV since 2009. The Burned area
449 dropped from 72% in 2011 to 35.46% in 2018, our year of measurements (Cardozo-Valencia et al., 2019).

450

451 Cd, Pb, Ni, Hg and As, and other metals and metalloids are considered carcinogenic (WHO Regional Office for Europe, 2020).
452 Measured concentrations of Pb and Ni in PM_{2.5} at Palmira were 18 ng m⁻³ (+/-19) and 2 ng m⁻³ (+/-1), respectively. These
453 mean values were below the EU target values of (0.5 µg m⁻³ and 20 ng m⁻³ respectively) (WHO, 2013a), and below the annual
454 average limit of the Colombian national ambient air quality standard (0.5 µg m⁻³ and 0.18 µg m⁻³ respectively) (MADS, 2017).
455 Nevertheless, these concentrations are significantly higher than those reported for other suburban areas in Midwestern United
456 States and remote sites in the northern tropical Atlantic (Fomba et al., 2018; Kundu and Stone, 2014). Pb concentrations are
457 similar to those reported for Bogota and other large urban areas (SDA, 2010; Vasconcellos et al., 2007). Pb has been long
458 banned as a fuel additive in Colombia, thus the observed levels might be associated with metallurgical industry and waste
459 incineration. Information on ambient air hazardous metal concentrations in Latin America's urban and rural areas is still scarce.

460

461 3.5. Carbohydrates

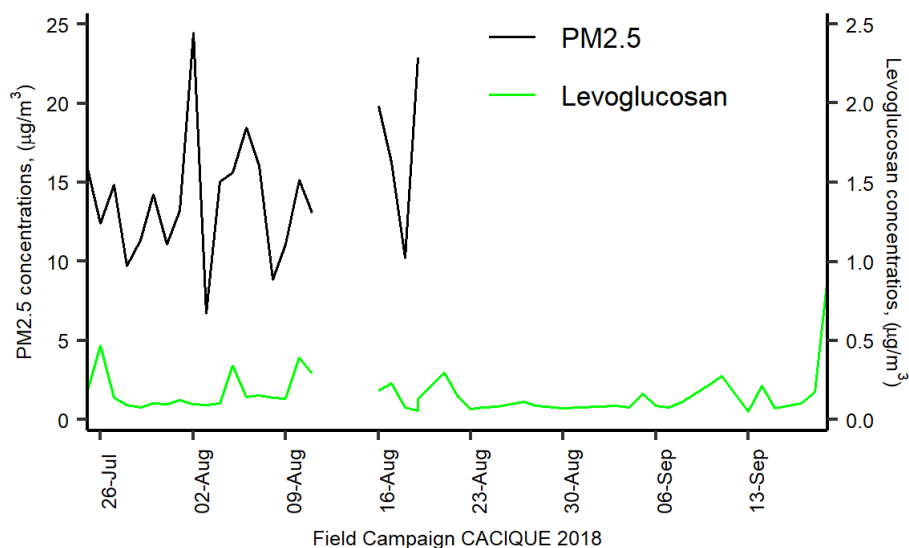
462

463 Levoglucosan is a highly specific biomass burning organic tracer (Bhattarai et al., 2019). Along with K⁺, OC and EC, it can
464 be used to effectively identify the relevance of biomass burning as an aerosol source. The relative contribution of levoglucosan
465 to the PM carbohydrate burden, and especially the levoglucosan to mannosan ratio, can be used as indicators of the type of
466 biomass burned (Engling et al., 2009). In this study, the following carbohydrates were quantified: levoglucosan, mannosan,
467 glucose, galactosan, fructose and arabitol. Levoglucosan was by far the most abundant (113.8 ± 147.2 ng m⁻³), reaching values
468 of up to 904.3 ng m⁻³, followed by glucose (10.4 ± 6.1 ng m⁻³), mannosan (7 ± 6.1 ng m⁻³), and arabitol (4.1 ± 3.5 ng m⁻³).
469 Levoglucosan and mannosan were detected in all PM_{2.5} samples, while galactosan and fructose were detected only in 9 and 11
470 samples, respectively. Levoglucosan was 3.5±2.3% of OC and 0.96% ± 0.81% of PM_{2.5}.

471

472 The levoglucosan concentration found in this study was quite similar to that reported in areas of Brazil where sugarcane
473 production and processing are important economic activities, Figure 3. For instance, during the harvest (*zafra*) period in
474 Araraquara, the levoglucosan mean concentration was 138 ± 91 ng m⁻³, although during the non-harvest period it was
475 unexpectedly high (73 ± 37 ng m⁻³) (Urban et al., 2014). Likewise, the levoglucosan average concentration at Piracicaba during
476 a reduced fire period was 66 ng m⁻³ (Souza et al., 2014). The measured mean levoglucosan/mannosan ratio in Palmira was 17.6
477 ± 13.0 (min: 8.1 – max: 58.1). Chemical profile studies found a levoglucosan/mannosan ratio of ~10 for sugarcane leaves
478 burned in stoves (Hall et al., 2012; Dos Santos et al., 2002) and of ~54 for burned bagasse (Dos Santos et al., 2002). Leaves
479 constitute the largest fraction (20.8%, Victoria et al., 2002) of pre-harvest burned sugarcane. Consistently and expectably, the
480 levoglucosan/mannosan ratio at Palmira is much closer to the chemical profile ratio of leaves than that of bagasse. Moreover,
481 ambient air samples in Araraquara and Piracicaba showed levoglucosan/mannosan ratios of 9 ± 5 and ~33, respectively. For
482 comparison, the levoglucosan/mannosan ratio in PM from rice straw and other crops burned were ~26.6 and ~23.8, respectively

483 (Engling et al., 2009). This indicates that the levoglucosan/mannosan ratio is sensitive to the type of biomass burned but also
 484 to burning conditions. The large levoglucosan/mannosan ratio in our study suggests that Palmira was impacted by sugarcane
 485 PHB most of the time, and, to a lesser extent, by bagasse combustion in sugar mills. We hypothesize that, even if these were
 486 very small, levoglucosan and mannosan combustion emissions might not be negligible as the CRV sugarcane biomass yields
 487 are very high and most of the harvested sugarcane bagasse is combusted for electric power and steam production.
 488



489

490

Figure 3. Daily variation of Levoglucosan and PM2.5 concentration at CRV.

491 3.6. Polycyclic Aromatic Hydrocarbons (PAH)

492

493 A total of 22 PAH were measured in each sample collected at Palmira, including the 16 PAH listed as human health priority
 494 pollutants by WHO and US-EPA (Yan et al., 2004). The total PAH concentration was $5.6 \pm 2.9 \text{ ng m}^{-3}$ (min: 2.3 ng m^{-3} – max:
 495 15.8 ng m^{-3}). Figure 4a shows the PAH concentration variability during the sampling campaign (mean and standard deviation
 496 are available in Table S2). The most abundant PAH were FLE ($44.2\% \pm 11.9\%$ total concentration share), ANT (9,10)
 497 ($10.0\% \pm 4.5\%$), BbF ($7.4\% \pm 2.3\%$), BghiP ($6.7\% \pm 2.4\%$), IcdP ($6.4\% \pm 1.9\%$), CPY ($6.0\% \pm 2.3\%$), FLO (9H) ($5.4\% \pm 3.1\%$),
 498 BeP ($4.6\% \pm 1.3\%$), and BaP ($4.4\% \pm 1.6\%$), which accounted for 95.1% of the total PAH concentration (Figure 4b). Three-ring
 499 PAHs were the most abundant (59.04% of total PAH). Put together, five- and six-ring PAHs accounted for an additional
 500 38.44%. The less abundant PAH group was the four-ring (2.52%). A previous study in CRV, carried out on PM_{10} samples by
 501 Romero et al. (2013), showed higher FLT, PYR, and PHE concentrations in areas highly exposed to sugarcane PHB compared
 502 to other locations. In contrast, $\text{PM}_{2.5}$ FLE concentrations in this research were significantly higher than those in PM_{10} by
 503 Romero et al. (2013), while PYR and PHE levels were similar.

504

505 The carcinogenic species BaP, BbF, BkF, BaA, BghiP, FLE, CPY and BeP were identified in all the PM_{2.5} samples. BaP is a
506 reference for PAH carcinogenicity (WHO, 2013a) that is used as a PAH exposure metric, known as the Benzo(a)Pyrene-
507 equivalent carcinogenic potency (BaPE). We calculated BaPE using the toxic equivalent factors (TEF) proposed by Nisbet
508 and LaGoy (1992) and (Malcolm and Dobson, 1994). PAH concentrations were multiplied by TEF and then added to estimate
509 the carcinogenic potential of PM_{2.5}-bound PAH. The mean carcinogenicity level at Palmira, expressed as BaP-TEQ, was 0.4
510 \pm 0.2 ng m⁻³ (min: 0.1 ng m⁻³ - max: 1.4 ng m⁻³). Only one sample exceeded the Colombian annual limit of 1 ng m⁻³ but most
511 of them exceeded the WHO reference level of 0.12 ng m⁻³. The mutagenic potential of PAH (BaP-MEQ) was estimated using
512 the mutagenic equivalent factors (MEF) reported by Durant et al., (1996). The average BaP-MEQ was 0.5 \pm 0.3 ng m⁻³ (min:
513 0.2 ng m⁻³ - max: 1.8 ng m⁻³). These levels are comparable to those measured in PM_{2.5} by Mugica-Álvarez et al., (2016) in
514 Veracruz (Mexico) but during the sugarcane non-harvest period. PM₁₀ BaP-MEQ levels in Araraquara (Brazil) (de Andrade et
515 al., 2010; De Assuncao et al., 2014) were twice as high as those found in this study. This suggests that year-long sugarcane
516 PHB in the CRV leads to lower mutagenic potentials compared to those at locations where the harvesting period (*zafra*) is
517 shorter, thus with higher burning rates. We estimated the average BaP-TEQ and BaP-MEQ concentrations in the CRV
518 according to their exposure to sugarcane burning products from Romero et al., (2013) data and used them as a benchmark to
519 our measurements. PM₁₀-bound BaP-TEQ and BaP-MEQ levels for areas not directly exposed to sugarcane burning were 0.16
520 ng m⁻³ and =0.21 ng m⁻³, respectively. Toxicity and mutagenicity due to PM₁₀-bound PAHs were 4 times as high as those at
521 areas directly exposed to sugarcane burning. It is reasonable to assume that PAHs are largely bound to fine aerosol (<2.5 μ m),
522 thus that our measurements are comparable to (Romero et al., 2013). If so, our site at Palmira would be at an intermediate
523 exposure condition, higher than areas not directly exposed to sugarcane burning but lower than directly exposed areas.

524

525 Ratios among different PAHs have been extensively used to distinguish between traffic and other PAH sources. We used the
526 diagnostic ratios presented by Ravindra et al. (2008) and Tobiszewski and Namieśnik (2012a) to better understand the
527 contribution of sources to PM_{2.5} in the CRV. The ratio benzo(e)pyrene to the sum of benzo(e)pyrene and benzo(a) pyrene is
528 used as an indicator of aerosol aging. Local or “fresh” aerosols have [BeP]/([BeP]+[BaP]) ratios around 0.5, while aged
529 aerosols can have ratios as low as zero as a result of photochemical decomposition and oxidation. The [BeP]/([BeP]+[BaP])
530 ratio at Palmira was 0.51 \pm 0.04, with a majority (84.4%, n = 38) of fresh samples a minor fraction (15.6%, n=7) of
531 photochemically-degraded samples.

532

533 Other two diagnostic ratios were used to assess the prevalence of traffic as a PM_{2.5} source. The first ratio used IcdP BghiP, two
534 automobile emissions markers (Miguel and Pereira, 1989). Values higher than 0.5 for the ratio [IdcP]/([IdcP]+[BghiP])
535 indicates aged particles (Tobiszewski and Namieśnik, 2012) generated by coal, grass or wood burning (Yunker et al., 2002).
536 The second ratio is [BaP]/[BghiP]. Ratios higher than 0.6 are indicative of traffic emissions (Tobiszewski and Namieśnik,

537 2012). At Palmira, the $[\text{IdcP}]/([\text{IdcP}]+[\text{BghiP}])$ and $[\text{BaP}]/[\text{BghiP}]$ ratios were 0.48 ± 0.04 and 0.69 ± 0.13 , which indicates
538 that ~63% of the samples originated from combustion of oil products ($n = 30$), and ~36% came from non-traffic sources, like
539 wood, grass, or coal ($n = 15$).

540

541 Also, the structure and size of PAHs are indicative of their sources. PAH of low molecular weight (LMW) (two or three
542 aromatic rings) have been reported as tracers of wood, grass, and fuel oil combustion, while those of medium molecular weight
543 (MMW) (four rings) and high molecular height (HMW) (five and six rings) are associated with coal combustion and vehicular
544 emissions. The ratio between LMW and the sum of MMW and HMW, $\text{LMW}/(\text{MMW}+\text{HMW})$, is used for source identification.
545 Ratios lower than one are indicative of oil products combustion, while ratios larger than one are associated with coal and
546 biomass combustion (Tobiszewski and Namieśnik, 2012). The ratio at Palmira, $\text{LMW}/(\text{MMW}+\text{HMW}) = 1.43 \pm 1.00$, was
547 rather variable but suggests that a large fraction of PAHs in CRV (82.2% of samples) were generated by biomass burning or
548 combustion, as coal combustion is quite limited nowadays. Just one in five samples (17.8%) had PAH attributable to oil product
549 combustion.

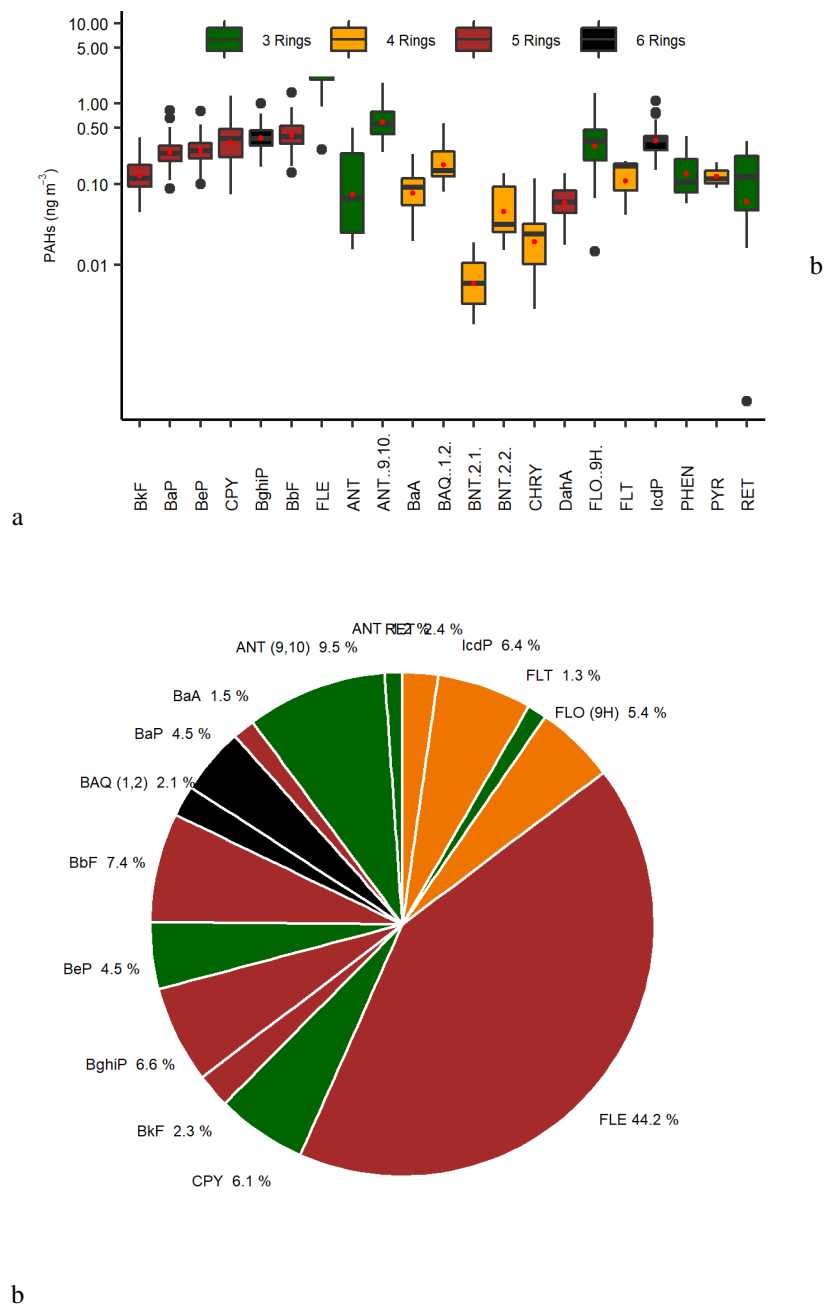
550

551 Sugarcane-burning emitted PAH are mainly LMW, especially of two (~66% of PAH) and three rings (~27%), among which
552 FLE, PHE and ANT are the most emitted, according to Hall et al. (2012) chemical profile. The relative abundance of three-
553 ring PAH (Figure 4) in CRV's $\text{PM}_{2.5}$ is likely due to open-field sugarcane PHB to a major extent, and to controlled bagasse
554 combustion for electric power and steam production, to a lesser extent.

555

556 The highest PAH concentrations were observed on 10th August and 11th September 2018, with levels of 15.8 ng m^{-3} and 14.4
557 ng m^{-3} , respectively (Fig 5S). Elevated concentrations of 5 and 6 ring PAH were observed on 10th August 2018. A change in
558 the wind circulation pattern was observed on the previous day (Fig S2), with a wind speed reduction and a predominance of
559 winds from the north. Later, on 11th September 2018, we observed an increase in 3-ring PAH and winds from the NW at the
560 average wind speed at the sampling location. This indicates that there were at least two types of sources. The abundance of
561 HMW PAH indicates fossil fuel combustion sources, and LMW PAH suggest that parts of these come from non-fossil fuel
562 combustion sources.

563



564 Figure 4. The abundance of PAH measured in PM_{2.5} samples collected in CRV, represented by colors according to the number
 565 of rings of each PAH, green (tree rings), yellow (four rings), brown (five rings), and black (six rings). a) Boxplot of
 566 concentrations in ng m⁻³, red dots represent mean concentrations of each PAH. b) pie-plot of the relative abundance of PAH
 567 in PM_{2.5} samples.

568 3.7. Alkanes

569

570 A total of 16 alkanes ranging from C₂₀ up to C₃₄ were analyzed in this study and used to identify the presence of fossil fuel
571 combustion and plant fragments in the PM_{2.5} samples. The abundance of total n-alkanes during the whole sampling period was
572 in the range of 13.0 to 88.45 ng m⁻³ with an average concentration of 40.36 ng m⁻³ ± 18.82 ng m⁻³. In general, the high molecular
573 weight n-alkanes such as C₂₉ – C₃₁ were the most abundant. These are characteristic of vegetative detritus corresponding to
574 plant fragments in airborne PM (Lin et al., 2010). The most abundant n-alkanes were C₂₉, C₃₀, and C₃₁ (Fig 6.). Likewise, the
575 carbon number maximum concentration (C_{max}) was C₂₉ in 43% of samples and C₃₁ in 28% of them. This result is consistent
576 with the chemical profile of sugarcane burning reported by (Oros et al., 2006) with a C_{max} of C₃₁.

577

578 The carbon preference index (CPI) and wax n-alkanes percentage (WNA%) are parameters used to elucidate the origin of the
579 n-alkanes and infer whether emissions come from biogenic or anthropogenic sources. The CPI represents the ratio between
580 odd and even carbon number n-alkanes. The equation used to calculate CPI in the present study is shown in Table 2, following
581 the procedure reported by (Marzi et al., 1993). Values of CPI ≤ 1 (or close to 1) indicate that n-alkanes are emitted from
582 anthropogenic sources, while values higher than 1 indicate the influence of vegetative detritus and biomass burning in the
583 PM_{2.5} samples (Mancilla et al., 2016). In this study, the mean CPI was always greater than 1, with an average value of 1.22 ±
584 0.18 (min:1.02 – max:1.8) that is between the CPI for fossil fuel emissions of ~1.0 (Caumo et al., 2020) and sugarcane burning
585 of 2.1 (Oros et al., 2006), revealing the influence of several sources over the PM_{2.5} in the CRV.

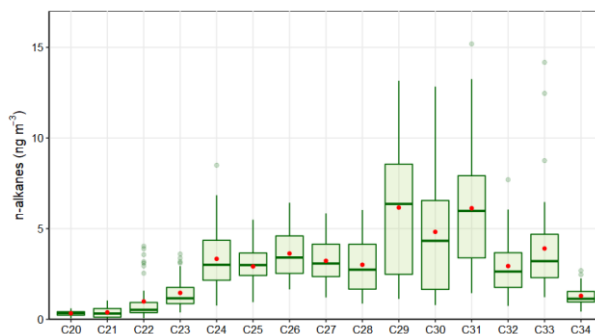
586

587 Likewise, WNA% represents the preference of odd n-alkanes in the sample. The odd n-alkanes, especially of higher molecular
588 weight, are representative of plant wax related emissions. The waxes are present on the surface of plants, especially on the
589 leaves, and they become airborne by a direct or indirect mechanism like wind action or biomass burning (Kang et al., 2018;
590 Simoneit, 2002). In this research, the samples analyzed showed a preference for odd carbon on C₂₇, C₂₉, C₃₁ and C₃₃, which
591 have higher concentrations than the next higher and lower even carbon number homologs, proving the biogenic contribution
592 over the PM_{2.5} in the CRV. The WNA% was calculated using the equation shown in Table 2, described by Yadav et al. (2013).
593 A larger WNA% represents the contribution from emissions of plant waxes or biomass burning. Otherwise, a smaller value
594 represents n-alkanes from petrogenic sources, known as petrogenic n-alkanes (PNA)%. The mean WNA% calculated for the
595 PM_{2.5} samples collected from the CRV was 12.65% ± 5.21% (min: 4.71% – max: 29.92%) and can be defined as petrogenic
596 inputs (PNA%) that were 87.35% during the sampling period. The correlation between CPI and WNA was moderate (r²=0.53)
597 supporting a consistent meaning between these two parameters, and they are useful for assessing the plant wax contribution to
598 PM_{2.5}.

599

600 Overall, the total concentration of n-alkanes in the PM_{2.5} in the CRV was lower than those reported in areas where sugarcane
 601 is often burned in Brazil (Urban et al., 2016), although the behavior of the parameters of CPI and C_{max} is similar. Compared
 602 with other urban areas in Latin America, the n-alkane concentration in the CRV was similar to that reported in the metropolitan
 603 zone of the Mexican valley (MZMV) for PM_{2.5} (Amador-Muñoz et al., 2011), Bogota for PM₁₀ and slightly lower than reported
 604 in Sao Paulo for PM₁₀ (Vasconcellos et al., 2011). However, the CPI and WNA in these cities were smaller than in the CRV,
 605 because of the strong influence of vehicular emissions in these densely populated cities. The OC/EC ratio was moderately
 606 associated with WNA values ($r^2 = 0.41$), indicating that an increase in this ratio can be explained by the vegetative detritus
 607 contribution to PM_{2.5}, while the levoglucosan concentrations did not show correspondence to the CPI and WNA values;
 608 therefore, the levoglucosan levels did not explain the preference of odd carbon number homologs. These results indicated that
 609 the n-alkanes found in this study came from several sources, with a noticeable contribution from plant wax emissions. The
 610 parameters used to assess the source contribution of PM_{2.5} through n-alkanes such as CPI and WNA%, were characteristic of
 611 aerosols collected in urban areas.

612



613

614

Figure 5. Average n-alkanes concentrations in PM_{2.5} samples

615 3.8. PM_{2.5} mass closure

616

617 Mass closure (Figure 6) shows the crucial contribution of organic material ($52.66 \pm 18.44\%$) and inorganic fraction, represented
 618 by sulfate ($12.69 \pm 2.84\%$), ammonium ($3.75 \pm 1.05\%$), nitrate ($2.56 \pm 1.29\%$). EC constituted $7.13 \pm 2.44\%$ of PM_{2.5}. The
 619 mineral fraction corresponded to dust ($3.51 \pm 1.35\%$) and TEO ($0.85 \pm 0.42\%$). Mass closure of $88.42 \pm 24.17\%$ was achieved.
 620 Although PM_{2.5} concentrations observed in the CRV were not so high as compared with those registered in Brazil and Mexico
 621 during the preharvest season, the EC percentage is in a similar range or slightly lower than those observed in other urban areas
 622 (Snider et al., 2016), showing the key role of incomplete combustion processes in the area.

623

624 The average (OC/EC) ratio found in CRV was 4.2 ± 0.72 , from which we can infer that secondary aerosol formation had a
 625 relevant role. The segregation of OC into the primary and secondary fractions was carried out using two methods. The first

626 was the EC tracer method applied in previous studies (Pio et al., 2011; Plaza et al., 2011), and the second was the organic
627 tracer method, which is based on the lineal regression between OC and organic tracers from primary sources. In the EC tracer
628 method, the $(OC/EC)_{\min}$ ratio selected to differentiate OC_{prim} from OC_{sec} was the minimum ratio observed, equivalent to 2.12.
629 Still, this value could induce the overestimation of OC_{prim} due to the distance between the emission sources and the sampling
630 site (27 m aboveground), and the local meteorological conditions that favor the volatilization and oxidation of organic
631 components into particles before being collected. As a result, OC_{prim} was estimated at 50.3% and OC_{sec} at 49.7% of the total
632 OC, with a minimum variability of 3.8%. The estimated OM_{pri} concentration was $3.22 \pm 1.09 \mu\text{g m}^{-3}$ and the OM_{sec}
633 concentration was $4.01 \pm 1.78 \mu\text{g m}^{-3}$, which represented 24.2% and 28.5% of $PM_{2.5}$ respectively.

634

635 In the organic tracer method, the contribution of fossil fuel combustion - mainly derived from transport -, biomass burning,
636 and vegetative detritus to OC_{prim} was estimated from a linear relationship between organic tracers and OC. Resulting
637 contributions were as follows: OC_{ff} : 16.38%, OC_{bb} : 15.19%, and OC_{det} : 1.45% of total OC measured. Overall, the use organic
638 tracer method to estimate OC_{prim} indicates that this carbonaceous fraction represents $32.68\% \pm 11.02\%$ of total OC, and it may
639 fluctuate between 17.61% and 68.60%.

640

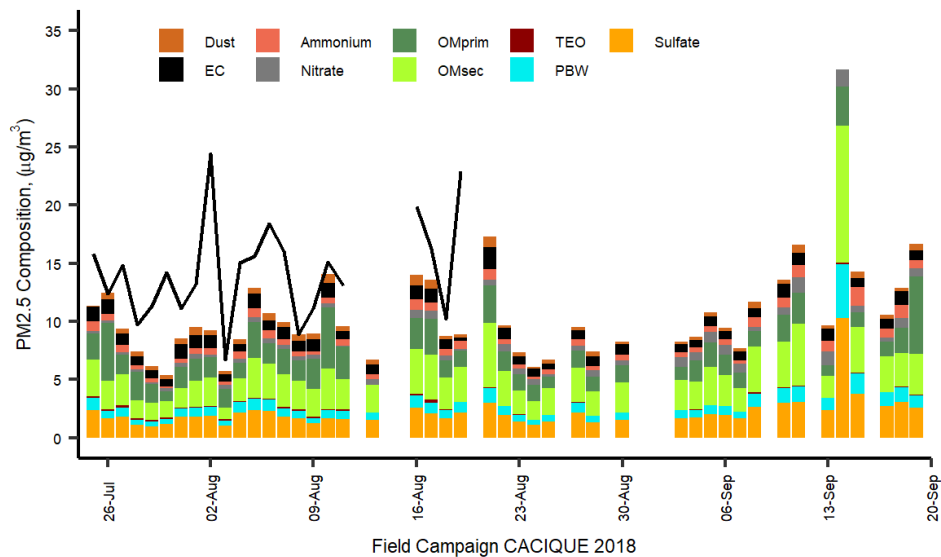
641 The difference between OC_{prim} from the organic tracer method and that obtained from the EC tracer method can be associated
642 to the fact that the organic tracer method may not be representative of all sources. Industrial coal and fuel oil burning, garbage
643 burning, cooking, charcoal production and other sources may not be accounted for by this method, since we did not have
644 specific organic tracers for each of these activities.

645

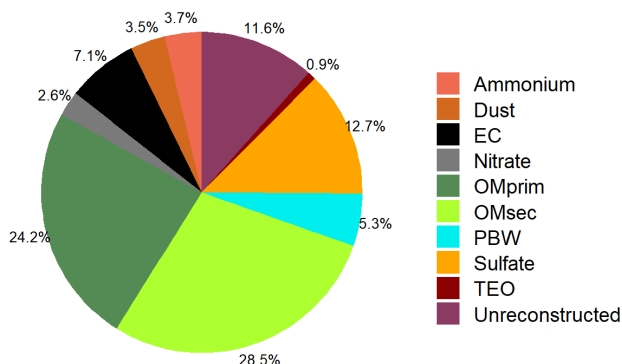
646 The mineral fraction, quantified as the sum of the oxides present in the crustal material (dust) and other TEO contributed $3.51 \pm$
647 1.35% and $0.85 \pm 0.42\%$, respectively. Despite the non-quantification of highly abundant mineral dust elements such as Si,
648 the concentrations of Ca, Ti, and Fe indicated the impact of soil resuspension on the $PM_{2.5}$ mass concentration.

649

650 PBW depends on the concentration of hygroscopic compounds embodied in the PM and the relative humidity of the weighing
651 room where $PM_{2.5}$ mass collected on the filters was determined. In this study, it was assumed that (i) NH_4^+ , SO_4^{2-} and NO_3^-
652 were the main compounds responsible for absorbed water and (ii) thermodynamic equilibrium is dominated by these ions that
653 allow calculating the H^+ molar fraction as a difference between $(\text{SO}_4^{2-} + \text{NO}_3^-)$ and NH_4^+ , which is required to establish charge
654 neutrality. Polar organic compounds and other water-soluble ions were not considered in the present study. The PBW content
655 was estimated using the mean measured concentrations of NH_4^+ , SO_4^{2-} and NO_3^- in the AIM Model, where a multiplier factor
656 of 0.32 was found as a proportion between the concentrations of the sum of these ions and the water fraction contained in
657 $PM_{2.5}$. As a result, PBW was 5.3% of the $PM_{2.5}$ mass concentration.



658



659

660 Figure 6. Mass reconstruction of PM_{2.5} collected in CRV. Figure in upper corresponding to timeseries of PM_{2.5} gravimetric
 661 mass measured and reconstructed mass from the chemical speciation in CRV during July – September 2018 and lower is the
 662 to pie plot the relative mean contributions (%) of major chemical components of gravimetric PM_{2.5} based on chemical
 663 speciation.

664

665 4. Conclusions

666 PM_{2.5} samples collected in the Cauca River Valley, Colombia, were analyzed to determine the main chemical components of
667 fine aerosol particles and to qualitatively identify aerosol sources using its chemical composition and diagnostic ratios. PM_{2.5}
668 during the campaign was $14.4 \pm 4.4 \mu\text{g m}^{-3}$. Its main components were OC ($4.0 \pm 1.3 \mu\text{g m}^{-3}$), sulfate ($2.2 \pm 1.4 \mu\text{g m}^{-3}$), and
669 EC ($1.0 \pm 0.3 \mu\text{g m}^{-3}$), ammonium ($0.7 \pm 0.6 \mu\text{g m}^{-3}$), and nitrate ($0.5 \pm 0.3 \mu\text{g m}^{-3}$). OM was estimated using the EC tracer
670 method and the organic tracer method. Mass closure using the EC tracer method explained 88.4% of PM_{2.5}, whereas the organic
671 tracer method explained 70.9% of PM_{2.5}. We attribute this difference to the lack of information of specific organic tracers for
672 some sources, both primary and secondary. Organic material and inorganic ions were the dominant groups of species,
673 constituting almost 79% of PM_{2.5}. OM_{prim} and OM_{sec} from the EC tracer method contribute 24.2% and 28.5% to PM_{2.5}.
674 Inorganic ions made up 19.0%, EC 7.1%, dust 3.5%, PBW 5.3%, and TEO 0.9% of PM_{2.5}.

675

676 Aerosol acidity was evaluated using three methods. The first, using the nitrate/sulfate ratio; the second using the anion/cation
677 equivalent ratio; and the third, estimating the pH with the E-AIM thermodynamic model. All methods showed that the aerosol
678 was acidic, with a pH of 2.5 ± 0.4 , mainly because of the abundance of organic and sulfur compounds.

679

680 Diagnostic ratios applied to organic compounds indicate that most PM_{2.5} was emitted locally and had contributions of both
681 pyrogenic and petrogenic sources. In addition, levoglucosan and mannosan levels showed that biomass burning was ubiquitous
682 during the sampling period. Fluoranthene (FLE) was the most abundant PAH, confirming the strong influence of BB associated
683 with agro-industry. Five- and six-ring PAH associated with vehicular emissions were also abundant in PM_{2.5}. Our
684 measurements point to BB as the main source of PAH in CRV. Relatively low PM_{2.5} concentrations and mutagenic potentials
685 are consistent with low-intensity, year-long BB and sugarcane PHB in CRV, which leads to lower atmospheric pollutant
686 burdens and mutagenic potentials compared to those at locations where the harvesting period is shorter (*zafra*) thus with higher
687 burning rates.

688 *Author contribution:* RJ, GR-S, and NR conceived and managed the project. LM-F, ACV-B, GR-S, and RJ set the instruments
689 up and performed the aerosol sampling. LM-F carried out the sample chemical analysis at TROPOS with the guidance and
690 support of DvP, MvP, KW, and HH. LM-F and ACV-B analyzed the measurement results, including PCA and other techniques
691 with the support of DvP and LM-F, RJ, NR and ACV-B prepared the manuscript with substantial contributions from all the
692 authors.

693 *Competing interests:* The authors declare that they have no conflict of interest.

694 *Acknowledgments:* The authors gratefully acknowledge the financial support from Universidad Nacional de Colombia – Sede
 695 Palmira (Project “Impacto de la quema de caña de azúcar en la calidad del aire del Valle Geografico del Río Cauca
 696 (CACIQUE), Hermes # 37718), and Leibniz Institute for Tropospheric Research (TROPOS) for analytical support. This
 697 project was supported by EU granted the mobility project PAPILA. We thank Susanne Fuchs, Anke Roedger, Sylvia
 698 Haferkorn, and Kornelia Pielok for their technical assistance in the chemical analysis of samples. We acknowledge Pablo
 699 Gutierrez for his contributions in the processing of the open sugarcane burning database and for preparing the CRV map.

700 **References**

701 Abdurrahman, M. I., Chaki, S. and Saini, G.: Stubble burning: Effects on health & environment, regulations and management
 702 practices, *Environ. Adv.*, 2(September), 100011, <https://doi.org/10.1016/j.envadv.2020.100011>, 2020.

703 Aerocivil: Estadísticas Operacionales, Operaciones aéreas Total. 2000-2019
 704 <https://www.aerocivil.gov.co/atencion/estadisticas-de-las-actividades-aeronauticas/estadisticas-operacionales>, last access: 15
 705 February 2022, 2019.

706 Agarwal, A., Satsangi, A., Lakhani, A. and Kumari, K. M.: Seasonal and spatial variability of secondary inorganic aerosols in
 707 PM_{2.5} at Agra: Source apportionment through receptor models, *Chemosphere*, 242, 125132,
 708 <https://doi.org/10.1016/j.chemosphere.2019.125132>, 2020.

709 Allen, A. G., Cardoso, A. A. and Da Rocha, G. O.: Influence of sugar cane burning on aerosol soluble ion composition in
 710 Southeastern Brazil, *Atmos. Environ.*, 38(30), 5025–5038, <https://doi.org/10.1016/j.atmosenv.2004.06.019>, 2004.

711 Alvi, M. U., Kistler, M., Shahid, I., Alam, K., Chishtie, F., Mahmud, T. and Kasper-Giebl, A.: Composition and source
 712 apportionment of saccharides in aerosol particles from an agro-industrial zone in the Indo-Gangetic Plain, *Environ. Sci. Pollut.*
 713 *Res.* 2020 2712, 27(12), 14124–14137, <https://doi.org/10.1007/S11356-020-07905-2>, 2020.

714 Amador-Muñoz, O., Villalobos-Pietrini, R., Miranda, J. and Vera-Avila, L. E.: Organic compounds of PM_{2.5} in Mexico
 715 Valley: Spatial and temporal patterns, behavior and sources, *Sci. Total Environ.*, 409(8), 1453–1465,
 716 <https://doi.org/10.1016/j.scitotenv.2010.11.026>, 2011.

717 Andrade, M. D. F., Miranda, R. M. De, Fornaro, A., Kerr, A., Oyama, B., Andre, P. A. De and Saldiva, P.: Vehicle emissions
 718 and PM_{2.5} mass concentrations in six Brazilian cities, *Air Qual. Atmos. Heal.*, 5, 79–88, [https://doi.org/10.1007/s11869-010-](https://doi.org/10.1007/s11869-010-0104-5)
 719 [0104-5](https://doi.org/10.1007/s11869-010-0104-5), 2012.

720 de Andrade, S. J., Cristale, J., Silva, F. S., Julião Zocolo, G. and Marchi, M. R. R.: Contribution of sugar-cane harvesting
 721 season to atmospheric contamination by polycyclic aromatic hydrocarbons (PAHs) in Araraquara city, Southeast Brazil,
 722 *Atmos. Environ.*, 44(24), 2913–2919, <https://doi.org/10.1016/j.atmosenv.2010.04.026>, 2010.

723 Andreae, M. O.: Soot Carbon and Excess Fine Potassium : Long-Range Transport of Combustion-Derived Aerosols., 1983.

724 Aneja, V. P., Schlesinger, W. H. and Erisman, J. W.: Farming pollution, *Nat. Geosci.*, 1(7), 409–411,
 725 <https://doi.org/10.1038/ngeo236>, 2008.

- 726 Aneja, V. P., Schlesinger, W. H. and Erisman, J. W.: Effects of agriculture upon the air quality and climate: Research, policy,
727 and regulations, *Environ. Sci. Technol.*, 43(12), 4234–4240, <https://doi.org/10.1021/es8024403>, 2009.
- 728 Asocaña: Aspectos Generales del Sector Agroindustrial de la Caña 2017 - 2018. Informe Anual. <https://www.asocana.org>,
729 2018.
- 730 Asocaña: Aspectos generales del sector agroindustrial de la caña Informe anual 2018-2019.
731 [https://www.asocana.org/documentos/2352019-D0CA1EED-](https://www.asocana.org/documentos/2352019-D0CA1EED-00FF00,000A000,878787,C3C3C3,0F0F0F,B4B4B4,FF00FF,2D2D2D,A3C4B5.pdf)
732 [00FF00,000A000,878787,C3C3C3,0F0F0F,B4B4B4,FF00FF,2D2D2D,A3C4B5.pdf](https://www.asocana.org/documentos/2352019-D0CA1EED-00FF00,000A000,878787,C3C3C3,0F0F0F,B4B4B4,FF00FF,2D2D2D,A3C4B5.pdf), last access: 20 May 2020, 2019.
- 733 Asocaña: Somos azucar y mucho más - Informe Anual 2019 - 2020., 2020.
- 734 De Assuncao, J. V., Pesquero, C. R., Nardocci, A. C., Francisco, A. P., Soares, N. S. and Ribeiro, H.: Airborne polycyclic
735 aromatic hydrocarbons in a medium-sized city affected by preharvest sugarcane burning and inhalation risk for human health,
736 *J. Air Waste Manag. Assoc.*, 64(10), 1130–1139, <https://doi.org/10.1080/10962247.2014.928242>, 2014.
- 737 Begam, G. R., Vachaspati, C. V., Ahammed, Y. N., Kumar, K. R., Reddy, R. R., Sharma, S. K., Saxena, M. and Mandal, T.
738 K.: Seasonal characteristics of water-soluble inorganic ions and carbonaceous aerosols in total suspended particulate matter at
739 a rural semi-arid site, Kadapa (India), *Environ. Sci. Pollut. Res.*, 24(2), 1719–1734, [https://doi.org/10.1007/s11356-016-7917-](https://doi.org/10.1007/s11356-016-7917-1)
740 1, 2016.
- 741 Bhattarai, H., Saikawa, E., Wan, X., Zhu, H., Ram, K., Gao, S., Kang, S., Zhang, Q., Zhang, Y., Wu, G., Wang, X., Kawamura,
742 K., Fu, P. and Cong, Z.: Levoglucosan as a tracer of biomass burning: Recent progress and perspectives, *Atmos. Res.*,
743 220(November 2018), 20–33, <https://doi.org/10.1016/j.atmosres.2019.01.004>, 2019.
- 744 Boman, J., Lindén, J., Thorsson, S., Holmer, B. and Eliasson, I.: A tentative study of urban and suburban fine particles (PM_{2.5})
745 collected in Ouagadougou, Burkina Faso, *X-Ray Spectrom.*, 38(4), 354–362, <https://doi.org/10.1002/XRS.1173>, 2009.
- 746 Cardozo-Valencia, A., Saa, G. R., Hernandez, A. J., Lopez, G. R. and Jimenez, R.: Distribución espaciotemporal y estimación
747 de emisiones por quema precosecha de caña de azúcar en el Valle del Cauca, *Conf. Proc. - Congr. Colomb. y Conf. Int. Calid.*
748 *Aire y Salud Publica, CASAP 2019*, <https://doi.org/10.1109/CASAP.2019.8916696>, 2019.
- 749 Casey, K. D., Bicudo, J. R., Schmidt, D. R., Singh, A., Gay, S. W., Gates, R. S., Jacobson, L. D. and Hoff, S. J.: Air quality
750 and emissions from livestock and poultry production / waste management systems, in *Animal Agriculture and the*
751 *Environment*, National Center for Manure & Animal Waste Management White Papers, pp. 1–40, , 2006.
- 752 Caumo, S., Bruns, R. E. and Vasconcellos, P. C.: Variation of the distribution of atmospheric n-alkanes emitted by different
753 fuels' combustion, *Atmosphere (Basel)*, 11(6), 1–19, <https://doi.org/10.3390/atmos11060643>, 2020.
- 754 Cavalli, F., Viana, M., Yttri, K. E., Genberg, J. and Putaud, J.: Toward a standardised thermal-optical protocol for measuring
755 atmospheric organic and elemental carbon: the EUSAAR protocol, *Atmos. Meas. Tech.*, 3, 79–89,
756 <https://doi.org/10.5194/amt-3-79-2010>, 2010.
- 757 Chen, J., Li, C., Ristovski, Z., Milic, A., Gu, Y., Islam, M. S., Wang, S., Hao, J., Zhang, H., He, C., Guo, H., Fu, H., Miljevic,
758 B., Morawska, L., Thai, P., LAM, Y. F., Pereira, G., Ding, A., Huang, X. and Dumka, U. C.: A review of biomass burning:

- 759 Emissions and impacts on air quality, health and climate in China, *Sci. Total Environ.*, 579(November 2016), 1000–1034,
760 <https://doi.org/10.1016/j.scitotenv.2016.11.025>, 2017.
- 761 Chow, J. C., Lowenthal, D. H., Chen, L. W. A., Wang, X. and Watson, J. G.: Mass reconstruction methods for PM_{2.5}: a
762 review, *Air Qual. Atmos. Heal.*, 8(3), 243–263, <https://doi.org/10.1007/s11869-015-0338-3>, 2015.
- 763 Clegg, S. L., Brimblecombe, P. and Wexler, A. S.: Thermodynamic Model of the System H⁺–NH₄⁺–SO₄²⁻–NO₃⁻–H₂O at
764 Tropospheric Temperatures, *J. Phys. Chem. A*, 102(12), 2137–2154, <https://doi.org/10.1021/jp973042r>, 1998.
- 765 Criollo, J. and Daza, N.: Evaluación de los niveles de concentración de metales en PM 10 producto de la quema de biomasa
766 en el valle geográfico del río Cauca, Universidad de la Salle, 2011.
- 767 Dabek-Zlotorzynska, E., Dann, T. F., Kalyani Martinelango, P., Celso, V., Brook, J. R., Mathieu, D., Ding, L. and Austin, C.
768 C.: Canadian National Air Pollution Surveillance (NAPS) PM_{2.5} speciation program: Methodology and PM_{2.5} chemical
769 composition for the years 2003–2008, *Atmos. Environ.*, 45(3), 673–686, <https://doi.org/10.1016/j.atmosenv.2010.10.024>,
770 2011.
- 771 Dajuma, A., Ogunjobi, K. O., Vogel, H., Knippertz, P., Siluś, S., N'Datchoh, E. T., Yoboué, V. and Vogel, B.: Downward
772 cloud venting of the central African biomass burning plume during the West Africa summer monsoon, *Atmos. Chem. Phys.*,
773 20(9), 5373–5390, <https://doi.org/10.5194/acp-20-5373-2020>, 2020.
- 774 Dávalos, E.: La caña de azúcar: ¿una amarga externalidad?, *Desarro. Soc.*, 59, 117–164, 2007.
- 775 Durant, J. L., Busby Jr, W. F., Lafleur, A. L., Penman, B. W. and Crespi, C. L.: Human cell mutagenicity of oxygenated,
776 nitrated and unsubstituted polycyclic aromatic hydrocarbons associated with urban aerosols, *Mutat. Res. - Genet. Toxicol.*,
777 371(3–4), 123–157, [https://doi.org/10.1016/S0165-1218\(96\)90103-2](https://doi.org/10.1016/S0165-1218(96)90103-2), 1996.
- 778 El-Zanan, H. S., Lowenthal, D. H., Zielinska, B., Chow, J. C. and Kumar, N.: Determination of the organic aerosol mass to
779 organic carbon ratio in IMPROVE samples, *Chemosphere*, 60(4), 485–496,
780 <https://doi.org/10.1016/j.chemosphere.2005.01.005>, 2005.
- 781 Engling, G., Lee, J. J., Tsai, Y.-W., Lung, S.-C. C., Chou, C. C.-K. and Chan, C.-Y.: Size-Resolved Anhydrosugar Composition
782 in Smoke Aerosol from Controlled Field Burning of Rice Straw, *Aerosol Sci. Technol.*, 43(7), 662–672,
783 <https://doi.org/10.1080/02786820902825113>, 2009.
- 784 FAO: FAOSTAT, <http://www.fao.org/faostat/en/#data/QC>, last access: 21 July 2021a, 2020.
- 785 FAO: FAOSTAT, <http://www.fao.org/faostat/en/#data/QC>, 2020b.
- 786 Fomba, K. ., Müller, K., Van Pinxteren, D. and Herrmann, H.: Aerosol size-resolved trace metal composition in remote
787 northern tropical Atlantic marine environment: case study Cape Verde islands, *Atmos. Chem. Phys.*, 13(9), 4801–4814,
788 <https://doi.org/10.5194/acp-13-4801-2013>, 2013.
- 789 Fomba, K. W., van Pinxteren, D., Müller, K., Spindler, G. and Herrmann, H.: Assessment of trace metal levels in size-resolved
790 particulate matter in the area of Leipzig, *Atmos. Environ.*, 176, <https://doi.org/10.1016/j.atmosenv.2017.12.024>, 2018.
- 791 Franzin, B. T., Guizzellini, F. C., de Babos, D. V., Hojo, O., Pastre, I. A., Marchi, M. R. R., Fertonani, F. L. and Oliveira, C.

- 792 M. R. R.: Characterization of atmospheric aerosol (PM₁₀ and PM_{2.5}) from a medium sized city in São Paulo state, Brazil, J.
793 Environ. Sci. (China), 89, 238–251, <https://doi.org/10.1016/j.jes.2019.09.014>, 2020.
- 794 Friese, E. and Ebel, A.: Temperature Dependent Thermodynamic Model of the System H + - NH₄ + - Na + - SO₄²⁻ - NO₃
795 - - Cl - - H₂O., 2010.
- 796 Gonçalves, C., Figueiredo, B. R., Alves, C. A., Cardoso, A. A. and Vicente, A. M.: Size-segregated aerosol chemical
797 composition from an agro-industrial region of São Paulo state, Brazil, Air Qual. Atmos. Heal. 2016 104, 10(4), 483–496,
798 <https://doi.org/10.1007/S11869-016-0441-0>, 2016.
- 799 Gondwe, M.: Comparison of modeled versus measured MSA: nss SO₄ = 4 ratios: A global analysis, , 18, 1–18,
800 <https://doi.org/10.1029/2003GB002144>, 2004.
- 801 H M Malcolm and Dobson, S.: The calculation of an Environmental Assessment Level (EAL) for atmospheric PAHs using
802 relative potencies., 1994.
- 803 Hall, D., Wu, C. Y., Hsu, Y. M., Stormer, J., Engling, G., Capeto, K., Wang, J., Brown, S., Li, H. W. and Yu, K. M.: PAHs,
804 carbonyls, VOCs and PM_{2.5} emission factors for pre-harvest burning of Florida sugarcane, Atmos. Environ., 55, 164–172,
805 <https://doi.org/10.1016/j.atmosenv.2012.03.034>, 2012.
- 806 He, C., Miljevic, B., Crilley, L. R., Surawski, N. C., Bartsch, J., Salimi, F., Uhde, E., Schnelle-Kreis, J., Orasche, J., Ristovski,
807 Z., Ayoko, G. A., Zimmermann, R. and Morawska, L.: Characterisation of the impact of open biomass burning on urban air
808 quality in Brisbane, Australia, Environ. Int., 91(x), 230–242, <https://doi.org/10.1016/j.envint.2016.02.030>, 2016.
- 809 Hernández, J. D. R. and Mesa, Ó. J.: A simple conceptual model for the heat induced circulation over Northern South America
810 and MESO-America, Atmosphere (Basel), 11(11), 1–14, <https://doi.org/10.3390/atmos11111235>, 2020.
- 811 Hopke, P. K.: Review of receptor modeling methods for source apportionment, J. Air Waste Manage. Assoc., 66(3), 237–259,
812 <https://doi.org/10.1080/10962247.2016.1140693>, 2016.
- 813 Ianniello, A., Spataro, F., Esposito, G., Allegrini, I., Hu, M. and Zhu, T.: and Physics Chemical characteristics of inorganic
814 ammonium salts in PM_{2.5} in the atmosphere of Beijing (China), , (October), <https://doi.org/10.5194/acp-11-10803-2011>,
815 2011.
- 816 IDEAM: 1er Inventario indicativo nacional de emisiones de contaminantes criterio & carbono negro 2010-2014, Bogotá D.C.,
817 2018.
- 818 Iinuma, Y., Engling, G., Puxbaum, H. and Herrmann, H.: A highly resolved anion-exchange chromatographic method for
819 determination of saccharidic tracers for biomass combustion and primary bio-particles in atmospheric aerosol, Atmos.
820 Environ., 43(6), 1367–1371, 2009.
- 821 Janta, R., Sekiguchi, K., Yamaguchi, R., Sopajaree, K., Pongpiachan, S. and Chetiyakornkul, T.: Ambient PM_{2.5}, polycyclic
822 aromatic hydrocarbons and biomass burning tracer in Mae Sot District, western Thailand, Atmos. Pollut. Res., 11(1), 27–39,
823 <https://doi.org/10.1016/j.apr.2019.09.003>, 2020.
- 824 Jenkins, B. M., Turn, S. Q. and Williams, R. B.: Atmospheric emissions from agricultural burning in California: Determination

- 825 of burn fractions, distribution factors, and crop-specific contributions, *Agric. Ecosyst. Environ.*, 38(4), 313–330,
826 [https://doi.org/10.1016/0167-8809\(92\)90153-3](https://doi.org/10.1016/0167-8809(92)90153-3), 1992.
- 827 Johnston, H. J., Mueller, W., Steinle, S., Vardoulakis, S., Tantrakarnapa, K., Loh, M. and Cherrie, J. W.: How Harmful Is
828 Particulate Matter Emitted from Biomass Burning? A Thailand Perspective, *Curr. Pollut. Reports*, 5(4), 353–377,
829 <https://doi.org/10.1007/s40726-019-00125-4>, 2019.
- 830 Jorquera, H. and Barraza, F.: Source apportionment of ambient PM_{2.5} in Santiago, Chile: 1999 and 2004 results, *Sci. Total*
831 *Environ.*, 435–436, 418–429, <https://doi.org/10.1016/j.scitotenv.2012.07.049>, 2012.
- 832 Jorquera, H. and Barraza, F.: Source apportionment of PM₁₀ and PM_{2.5} in a desert region in northern Chile, *Sci. Total*
833 *Environ.*, 444, 327–335, <https://doi.org/10.1016/j.scitotenv.2012.12.007>, 2013.
- 834 Kang, M., Ren, L., Ren, H., Zhao, Y., Kawamura, K., Zhang, H., Wei, L., Sun, Y., Wang, Z. and Fu, P.: Primary biogenic and
835 anthropogenic sources of organic aerosols in Beijing, China: Insights from saccharides and n-alkanes, *Environ. Pollut.*, 243,
836 1579–1587, <https://doi.org/10.1016/j.envpol.2018.09.118>, 2018.
- 837 Karagulian, F., Belis, C. A., Francisco, C., Dora, C., Prüss-ustün, A. M., Bonjour, S., Adair-rohani, H. and Amann, M.:
838 Contributions to cities ' ambient particulate matter (PM): A systematic review of local source contributions at global level,
839 *Atmos. Environ.*, 120, 475–483, <https://doi.org/10.1016/j.atmosenv.2015.08.087>, 2015.
- 840 Khedidji, S., Müller, K., Rabhi, L., Spindler, G., Fomba, K. W., Pinxteren, D. van, Yassaa, N. and Herrmann, H.: Chemical
841 Characterization of Marine Aerosols in a South Mediterranean Coastal Area Located in Bou Ismaïl, Algeria, *Aerosol Air Qual.*
842 *Res.*, 20(January), <https://doi.org/10.4209/aaqr.2019.09.0458>, 2020.
- 843 Kundu, S. and Stone, E. A.: Composition and sources of fine particulate matter across urban and rural sites in the Midwestern
844 United States, *Environ. Sci. Process. Impacts*, 16(6), 1360–1370, <https://doi.org/10.1039/c3em00719g>, 2014.
- 845 Kuo, C. Y., Chien, P. S., Kuo, W. C., Wei, C. T. and Rau, J. Y.: Comparison of polycyclic aromatic hydrocarbon emissions
846 on gasoline- and diesel-dominated routes, *Environ. Monit. Assess.*, 185(7), 5749–5761, [https://doi.org/10.1007/s10661-012-](https://doi.org/10.1007/s10661-012-2981-6)
847 2981-6, 2013.
- 848 Lara, L. L., Artaxo, P., Martinelli, L. A., Camargo, P. B., Victoria, R. L. and Ferraz, E. S. B.: Properties of aerosols from
849 sugar-cane burning emissions in Southeastern Brazil, *Atmos. Environ.*, 39(26), 4627–4637,
850 <https://doi.org/10.1016/j.atmosenv.2005.04.026>, 2005.
- 851 Lee, S., Wang, Y. and Russell, A. G.: Assessment of secondary organic carbon in the southeastern United States: A review, *J.*
852 *Air Waste Manag. Assoc.*, 60(11), 1282–1292, <https://doi.org/10.3155/1047-3289.60.11.1282>, 2010.
- 853 Lee, T., Yu, X., Kreidenweis, S. M., Malm, W. C. and Collett, J. L.: Semi-continuous measurement of PM_{2.5} ionic
854 composition at several rural locations in the United States, , 42, 6655–6669, <https://doi.org/10.1016/j.atmosenv.2008.04.023>,
855 2008.
- 856 Li, F., Zhang, X. and Kondragunta, S.: Biomass burning in Africa: An investigation of fire radiative power missed by MODIS
857 using the 375 m VIIRS active fire product, *Remote Sens.*, 12(10), <https://doi.org/10.3390/rs12101561>, 2020.

- 858 Li, J., Song, Y., Mao, Y., Mao, Z., Wu, Y., Li, M., Huang, X., He, Q. and Hu, M.: Chemical characteristics and source
859 apportionment of PM_{2.5} during the harvest season in eastern China's agricultural regions, *Atmos. Environ.*, 92, 442–448,
860 <https://doi.org/10.1016/J.ATMOSENV.2014.04.058>, 2014.
- 861 Li, X., Wang, L., Ji, D., Wen, T., Pan, Y., Sun, Y. and Wang, Y.: Characterization of the size-segregated water-soluble
862 inorganic ions in the Jing-Jin-Ji urban agglomeration: Spatial/temporal variability, size distribution and sources, *Atmos.*
863 *Environ.*, 77, 250–259, <https://doi.org/10.1016/j.atmosenv.2013.03.042>, 2013.
- 864 Liang, C. S., Duan, F. K., He, K. Bin and Ma, Y. L.: Review on recent progress in observations, source identifications and
865 countermeasures of PM_{2.5}, *Environ. Int.*, 86, 150–170, <https://doi.org/10.1016/j.envint.2015.10.016>, 2016.
- 866 Lin, L., Lee, M. L. and Eatough, D. J.: Review of recent advances in detection of organic markers in fine particulate matter
867 and their use for source apportionment, *J. Air Waste Manag. Assoc.*, 60(1), 3–25, <https://doi.org/10.3155/1047-3289.60.1.3>,
868 2010.
- 869 López Larada, J.: |Zona portuaria de Buenaventura: y su importancia en Colombia, Univ. San Buenaventura, 1–14
870 http://bibliotecadigital.usbcali.edu.co/bitstream/10819/7099/1/Zona_Portuaria_Buenaventura_Lopez_2017.pdf, last access:
871 23 February 2022, 2017.
- 872 Lopez, M. and Howell, W.: Katabatic Winds in the equatorial Andes, *J. Atmos. Sci.*, 24(1), 29–35, 1967.
- 873 Lyu, R., Shi, Z., Alam, M. S., Wu, X., Liu, D., Vu, T. V., Stark, C., Xu, R., Fu, P., Feng, Y. and Harrison, R. M.: Alkanes and
874 aliphatic carbonyl compounds in wintertime PM_{2.5} in Beijing, China, *Atmos. Environ.*, 202(November 2018), 244–255,
875 <https://doi.org/10.1016/j.atmosenv.2019.01.023>, 2019.
- 876 MADS: Res. No 2254, Ministerio de Ambiente y Desarrollo Sostenible, Colombia., 2017.
- 877 Majra, J. P.: Air Quality in Rural Areas, in *Chemistry, Emission Control, Radioactive Pollution and Indoor Air Quality*,
878 <https://doi.org/10.5772/16890>, , 2011.
- 879 Mancilla, Y., Mendoza, A., Fraser, M. P. and Herckes, P.: Organic composition and source apportionment of fine aerosol at
880 Monterrey, Mexico, based on organic markers, *Atmos. Chem. Phys.*, 16(2), 953–970, [https://doi.org/10.5194/acp-16-953-](https://doi.org/10.5194/acp-16-953-2016)
881 2016, 2016.
- 882 Marzi, R., Torkelson, B. E. and Olson, R. K.: A revised carbon preference index, *Org. Geochem.*, 20(8), 1303–1306,
883 [https://doi.org/10.1016/0146-6380\(93\)90016-5](https://doi.org/10.1016/0146-6380(93)90016-5), 1993.
- 884 Mesa S., Ó. J. and Rojo H., J. D.: On the general circulation of the atmosphere around Colombia, *Rev. la Acad. Colomb.*
885 *Ciencias Exactas, Fis. y Nat.*, 44(172), 857–875, <https://doi.org/10.18257/RACCEFYN.899>, 2020.
- 886 Miguel, A. H. and Pereira, P. A. P.: Benzo(k)fluoranthene, benzo(ghi)perylene, and indeno(1, 2, 3-cd)pyrene: New tracers of
887 automotive emissions in receptor modeling, *Aerosol Sci. Technol.*, 10(2), 292–295,
888 <https://doi.org/10.1080/02786828908959265>, 1989.
- 889 Min.Agricultura: Cadenas cárnicas bovina - bufalina, Bogotá D.C.
890 [https://sioc.minagricultura.gov.co/Bovina/Documentos/2018-12-30 Cifras Sectoriales.pdf](https://sioc.minagricultura.gov.co/Bovina/Documentos/2018-12-30%20Cifras%20Sectoriales.pdf), 2018.

- 891 Min.Agricultura: Cadena Carnica Porcina, Bogotá D.C. <https://sioc.minagricultura.gov.co/Porcina/Documentos/2019-12-30>
892 Cifras sectoriales.pdf, 2019.
- 893 Min.Agricultura: Cadena Avícola, segundo trimestre 2020, Bogotá D.C.
894 <https://www.minagricultura.gov.co/paginas/default.aspx>, 2020.
- 895 Mkoma, S. L., Kawamura, K. and Fu, P. Q.: Contributions of biomass/biofuel burning to organic aerosols and particulate
896 matter in Tanzania, East Africa, based on analyses of ionic species, organic and elemental carbon, levoglucosan and mannosan,
897 *Atmos. Chem. Phys.*, 13(20), 10325–10338, <https://doi.org/10.5194/acp-13-10325-2013>, 2013.
- 898 Mugica-Alvarez, V., Santiago-de la Rosa, N., Figueroa-Lara, J., Flores-Rodríguez, J., Torres-Rodríguez, M. and Magaña-
899 Reyes, M.: Emissions of PAHs derived from sugarcane burning and processing in Chiapas and Morelos México, *Sci. Total*
900 *Environ.*, 527–528, 474–482, <https://doi.org/10.1016/j.scitotenv.2015.04.089>, 2015.
- 901 Mugica-Álvarez, V., Ramos-Guizar, S., Santiago-de la Rosa, N., Torres-Rodríguez, M. and Noreña-Franco, L.: Black Carbon
902 and Particulate Organic Toxics Emitted by Sugarcane Burning in Veracruz, México, *Int. J. Environ. Sci. Dev.*, 7(4), 290–294,
903 <https://doi.org/10.7763/ijesd.2016.v7.786>, 2016.
- 904 Mugica-Álvarez, V., Hernández-Rosas, F., Magaña-Reyes, M., Herrera-Murillo, J., Santiago-De La Rosa, N., Gutiérrez-
905 Arzaluz, M., de Jesús Figueroa-Lara, J. and González-Cardoso, G.: Sugarcane burning emissions: Characterization and
906 emission factors, *Atmos. Environ.*, 193, 262–272, <https://doi.org/10.1016/j.atmosenv.2018.09.013>, 2018.
- 907 Murillo, J. H., Roman, S. R., Felix, J., Marin, R., Ramos, A. C., Jimenez, S. B., Gonzalez, B. C. and Baumgardner, D. G.:
908 Chemical characterization and source apportionment of PM10 and PM2.5 in the metropolitan area of Costa Rica, *Central*
909 *America Jorge, Atmos. Pollut. Res.*, 4(2), 181–190, <https://doi.org/10.5094/APR.2013.018>, 2013.
- 910 Neusüss, C., Pelzing, M., Plewka, A. and Herrmann, H.: A new analytical approach for size-resolved speciation of organic
911 compounds in atmospheric aerosol particles: Methods and first results, *J. Geophys. Res. Atmos.*, 105(D4), 4513–4527,
912 <https://doi.org/10.1029/1999JD901038>, 2000.
- 913 Nisbet, I. C. T. and LaGoy, P. K.: Toxic equivalency factors (TEFs) for polycyclic aromatic hydrocarbons (PAHs), *Regul.*
914 *Toxicol. Pharmacol.*, 16(3), 290–300, [https://doi.org/10.1016/0273-2300\(92\)90009-X](https://doi.org/10.1016/0273-2300(92)90009-X), 1992.
- 915 Oros, D. R., Abas, M. R. bin, Omar, N. Y. M. J., Rahman, N. A. and Simoneit, B. R. T.: Identification and emission factors of
916 molecular tracers in organic aerosols from biomass burning: Part 3. Grasses, *Appl. Geochemistry*, 21(6), 919–940,
917 <https://doi.org/10.1016/j.apgeochem.2006.01.008>, 2006.
- 918 Orozco, C., Sanandres, E. and Molineras, I.: Colombia, Panamá y la Ruta Panamericana: Encuentros y Desencuentros,
919 *Memorias Rev. Digit. Hist. y Arqueol. desde el Caribe*, 16(ISSN 1794-8886)
920 http://www.scielo.org.co/scielo.php?script=sci_arttext&pid=S1794-88862012000100005, last access: 23 February 2022,
921 2012.
- 922 Ortiz, E. Y., Jimenez, R., Fochesatto, G. J. and Morales-Rincon, L. A.: Caracterización de la turbulencia atmosférica en una
923 gran zona verde de una megaciudad andina tropical, *Rev. la Acad. Colomb. Ciencias Exactas, Físicas y Nat.*, 43(166), 133,

- 924 <https://doi.org/10.18257/raccefyn.697>, 2019.
- 925 Pan, X., Ichoku, C., Chin, M., Bian, H., Darmenov, A., Colarco, P., Ellison, L., Kucsera, T., Da Silva, A., Wang, J., Oda, T.
926 and Cui, G.: Six global biomass burning emission datasets: Intercomparison and application in one global aerosol model,
927 *Atmos. Chem. Phys.*, 20(2), 969–994, <https://doi.org/10.5194/acp-20-969-2020>, 2020.
- 928 Pant, P. and Harrison, R. M.: Estimation of the contribution of road traffic emissions to particulate matter concentrations from
929 field measurements: A review, *Atmos. Environ.*, 77, 78–97, <https://doi.org/10.1016/j.atmosenv.2013.04.028>, 2013.
- 930 Pereira, G. M., Teinilä, K., Custódio, D., Gomes Santos, A., Xian, H., Hillamo, R., Alves, C. A., Bittencourt de Andrade, J.,
931 Olímpio da Rocha, G., Kumar, P., Balasubramanian, R., Andrade, M. de F. and de Castro Vasconcellos, P.: Particulate
932 pollutants in the Brazilian city of São Paulo: 1-year investigation for the chemical composition and source apportionment,
933 *Atmos. Chem. Phys.*, 17(19), 11943–11969, <https://doi.org/10.5194/acp-17-11943-2017>, 2017.
- 934 Pereira, G. M., Oraggio, B., Teinilä, K., Custódio, D., Huang, X., Hillamo, R., Alves, C. A., Balasubramanian, R., Rojas, N.
935 Y. and Sanchez-Ccoyllo, O.: A comparative chemical study of PM 10 in three Latin American cities : Lima, Medellín, ans São
936 Paulo, *Air Qual. Atmos. Heal.*, 12, 1141–1152, <https://doi.org/10.1007/s11869-019-00735-3>, 2019.
- 937 Pio, C., Cerqueira, M., Harrison, R. M., Nunes, T., Mirante, F., Alves, C., Oliveira, C., Sanchez de la Campa, A., Artñano, B.
938 and Matos, M.: OC/EC ratio observations in Europe: Re-thinking the approach for apportionment between primary and
939 secondary organic carbon, *Atmos. Environ.*, 45(34), 6121–6132, <https://doi.org/10.1016/j.atmosenv.2011.08.045>, 2011.
- 940 Plaza, J., Artñano, B., Salvador, P., Gómez-Moreno, F. J., Pujadas, M. and Pio, C. A.: Short-term secondary organic carbon
941 estimations with a modified OC/EC primary ratio method at a suburban site in Madrid (Spain), *Atmos. Environ.*, 45(15), 2496–
942 2506, <https://doi.org/10.1016/j.atmosenv.2011.02.037>, 2011.
- 943 Pongpiachan, S., Hattayanone, M. and Cao, J.: Effect of agricultural waste burning season on PM2.5-bound polycyclic
944 aromatic hydrocarbon (PAH) levels in Northern Thailand, *Atmos. Pollut. Res.*, 8(6), 1069–1080,
945 <https://doi.org/10.1016/j.apr.2017.04.009>, 2017.
- 946 Pye, H. O. T., Nenes, A., Alexander, B., Ault, A. P., Barth, M. C., Clegg, S. L., Collett, J. L., Fahey, K. M., Hennigan, C. J.,
947 Herrmann, H., Kanakidou, M., Kelly, J. T., Ku, I. T., Faye McNeill, V., Riemer, N., Schaefer, T., Shi, G., Tilgner, A., Walker,
948 J. T., Wang, T., Weber, R., Xing, J., Zaveri, R. A. and Zuend, A.: The acidity of atmospheric particles and clouds., 2020.
- 949 Ramírez, O., Sánchez de la Campa, A. M., Amato, F., Catacolí, R. A., Rojas, N. Y. and de la Rosa, J.: Chemical composition
950 and source apportionment of PM10 at an urban background site in a high–altitude Latin American megacity (Bogota,
951 Colombia), *Environ. Pollut.*, 233, 142–155, <https://doi.org/10.1016/j.envpol.2017.10.045>, 2018.
- 952 Ravindra, K., Sokhi, R. and Van Grieken, R.: Atmospheric polycyclic aromatic hydrocarbons: Source attribution, emission
953 factors and regulation, *Atmos. Environ.*, 42(13), 2895–2921, <https://doi.org/10.1016/j.atmosenv.2007.12.010>, 2008.
- 954 Romero, D., Sarmiento, H. and Pachón, J. E.: Estimación de hidrocarburos aromáticos policíclicos y metales pesados asociados
955 con la quema de caña de azúcar en el valle geográfico del río Cauca , Colombia, *Rev. Épsilon*, 21(2013), 57–82, 2013.
- 956 Ryu, S. Y., Kim, J. E., Zhuanshi, H., Kim, Y. J. and Kang, G. U.: Chemical composition of post-harvest biomass burning

- 957 aerosols in gwangju, Korea, *J. Air Waste Manag. Assoc.*, 54(9), 1124–1137,
958 <https://doi.org/10.1080/10473289.2004.10471018>, 2004.
- 959 Dos Santos, C. Y. M., Azevedo, D. de A. and De Aquino Neto, F. R.: Selected organic compounds from biomass burning
960 found in the atmospheric particulate matter over sugarcane plantation areas, *Atmos. Environ.*, 36(18), 3009–3019,
961 [https://doi.org/10.1016/S1352-2310\(02\)00249-2](https://doi.org/10.1016/S1352-2310(02)00249-2), 2002.
- 962 Schauer, J. J.: Sources contributions to atmospheric organic compound concentrations: Emissions measurements and model
963 predictions, California Institute Technology, 1998.
- 964 SDA: Plan decenal de descontaminación del aire de Bogotá, Bogotá D.C.
965 [http://ambientebogota.gov.co/en/c/document_library/get_file?uuid=b5f3e23f-9c5f-40ef-912a-](http://ambientebogota.gov.co/en/c/document_library/get_file?uuid=b5f3e23f-9c5f-40ef-912a-51a5822da320&groupId=55886)
966 [51a5822da320&groupId=55886](http://ambientebogota.gov.co/en/c/document_library/get_file?uuid=b5f3e23f-9c5f-40ef-912a-51a5822da320&groupId=55886), 2010.
- 967 Seinfeld, J. H. and Pandis, S. N.: *Atmospheric From Air Pollution to Climate Change.*, 2006.
- 968 SICOM: Boletín estadístico, Boletín Estad. EDS automotriz y Fluv. <https://www.sicom.gov.co/index.php/boletin-estadistico>,
969 last access: 15 February 2022, 2018.
- 970 Simoneit, B. R. T.: Biomass burning - A review of organic tracers for smoke from incomplete combustion, *Appl.*
971 *Geochemistry*, 17(3), 129–162, [https://doi.org/10.1016/S0883-2927\(01\)00061-0](https://doi.org/10.1016/S0883-2927(01)00061-0), 2002.
- 972 Snider, G., Weagle, C. L., Murdymootoo, K. K., Ring, A., Ritchie, Y., Stone, E., Walsh, A., Akoshile, C., Anh, N. X.,
973 Balasubramanian, R., Brook, J., Qonitan, F. D., Dong, J., Griffith, D., He, K., Holben, B. N., Kahn, R., Lagrosas, N., Lestari,
974 P., Ma, Z., Misra, A., Norford, L. K., Quel, E. J., Salam, A., Schichtel, B., Segev, L., Tripathi, S., Wang, C., Yu, C., Zhang,
975 Q., Zhang, Y., Brauer, M., Cohen, A., Gibson, M. D., Liu, Y., Martins, J. V., Rudich, Y. and Martin, R. V.: Variation in global
976 chemical composition of PM_{2.5}: emerging results from SPARTAN, *Atmos. Chem. Phys.*, 16(15), 9629–9653,
977 <https://doi.org/10.5194/acp-16-9629-2016>, 2016.
- 978 Sorooshian, A., Crosbie, E., Maudlin, L. C., Youn, J., Wang, Z., Shingler, T., Ortega, A. M., Hersey, S. and Woods, R. K.:
979 Surface and airborne measurements of organosulfur and methanesulfonate over the western United States and coastal areas, *J.*
980 *Geophys. Res. Atmos.*, 8535–8548, <https://doi.org/10.1002/2015JD023822>.Received, 2015.
- 981 Souza, D. Z., Vasconcellos, P. C., Lee, H., Aurela, M., Saarnio, K., Teinilä, K. and Hillamo, R.: Composition of PM_{2.5} and
982 PM₁₀ collected at Urban Sites in Brazil, *Aerosol Air Qual. Res.*, 14(1), 168–176, <https://doi.org/10.4209/aaqr.2013.03.0071>,
983 2014.
- 984 Sutton, M. A., Billen, G., Bleeker, A., Erisman, J. W., Grennfelt, P., Grinsven, H. Van, Grizzetti, B., Howard, C. M. and Leip,
985 A.: Technical summary Part I Nitrogen in Europe : the present position, *Eur. Nitrogen Assess. Sources, Eff. Policy Perspect.*,
986 (December 2015), Xxxv–Lii, <https://doi.org/10.1017/CBO9780511976988.003>, 2011.
- 987 Szabó, J., Szabó Nagy, A. and Erdős, J.: Ambient concentrations of PM₁₀, PM₁₀-bound polycyclic aromatic hydrocarbons
988 and heavy metals in an urban site of Győr, Hungary, *Air Qual. Atmos. Heal.*, 8(2), 229–241, [https://doi.org/10.1007/s11869-](https://doi.org/10.1007/s11869-015-0318-7)
989 [015-0318-7](https://doi.org/10.1007/s11869-015-0318-7), 2015.

- 990 Tang, M., Guo, L., Bai, Y., Huang, R., Wu, Z. and Wang, Z.: Impacts of methanesulfonate on the cloud condensation
991 nucleation activity of sea salt aerosol, *Atmos. Environ.*, 201(October 2018), 13–17,
992 <https://doi.org/10.1016/j.atmosenv.2018.12.034>, 2019.
- 993 Tobiszewski, M. and Namieśnik, J.: PAH diagnostic ratios for the identification of pollution emission sources, *Environ. Pollut.*,
994 162(November 2018), 110–119, <https://doi.org/10.1016/j.envpol.2011.10.025>, 2012.
- 995 Turpin, B. J. and Lim, H.: Species Contributions to PM_{2.5} Mass Concentrations : Revisiting Common Assumptions for
996 Estimating Organic Mass, *Aerosol Sci. Technol.*, 35:1(September 2014), 37–41,
997 <https://doi.org/http://dx.doi.org/10.1080/02786820119445>, 2010.
- 998 Urban, R. C., Lima-Souza, M., Caetano-Silva, L., Queiroz, M. E. C., Nogueira, R. F. P., Allen, A. G., Cardoso, A. A., Held,
999 G. and Campos, M. L. A. M.: Use of levoglucosan, potassium, and water-soluble organic carbon to characterize the origins of
1000 biomass-burning aerosols, *Atmos. Environ.*, 61, 562–569, <https://doi.org/10.1016/j.atmosenv.2012.07.082>, 2012.
- 1001 Urban, R. C., Alves, C. A., Allen, A. G., Cardoso, A. A., Queiroz, M. E. C. and Campos, M. L. A. M.: Sugar markers in aerosol
1002 particles from an agro-industrial region in Brazil, *Atmos. Environ.*, 90(2014), 106–112,
1003 <https://doi.org/10.1016/j.atmosenv.2014.03.034>, 2014.
- 1004 Urban, R. C., Alves, C. A., Allen, A. G., Cardoso, A. A. and Campos, M. L. A. M.: Organic aerosols in a Brazilian agro-
1005 industrial area: Speciation and impact of biomass burning, *Atmos. Res.*, 169, 271–279,
1006 <https://doi.org/10.1016/j.atmosres.2015.10.008>, 2016.
- 1007 Vargas, F. A., Rojas, N. Y., Pachon, J. E. and Russell, A. G.: PM₁₀ characterization and source apportionment at two
1008 residential areas in Bogota, *Atmos. Pollut. Res.*, 3(1), 72–80, <https://doi.org/10.5094/APR.2012.006>, 2012.
- 1009 Vasconcellos, P. C., Balasubramanian, R., Bruns, R. E., Sanchez-Ccoyllo, O., Andrade, M. F. and Flues, M.: Water-soluble
1010 ions and trace metals in airborne particles over urban areas of the state of São Paulo, Brazil: Influences of local sources and
1011 long range transport, *Water. Air. Soil Pollut.*, 186(1–4), 63–73, <https://doi.org/10.1007/s11270-007-9465-2>, 2007.
- 1012 Vasconcellos, P. C., Souza, D. Z., Ávila, S. G., Araújo, M. P., Naoto, E., Nascimento, K. H., Cavalcante, F. S., Dos, M.,
1013 Smichowski, P. and Behrentz, E.: Comparative study of the atmospheric chemical composition of three South American cities,
1014 *Atmos. Environ.*, 45(32), 5770–5777, <https://doi.org/10.1016/j.atmosenv.2011.07.018>, 2011.
- 1015 Victoria, J., Amaya, A., Rangel, H., Viveros, C., Cassalet, C., Carbonell, J., Quintero, R., Cruz, R., Isaacs, C., Larrahondo, J.,
1016 Moreno, C., Palma, A., Posada, C., Villegas, F. and Gómez, L.: Características agronómicas y de productividad de la variedad
1017 Cenicaña Colombiana (CC) 85-92, Cali., 2002.
- 1018 Villalobos, A. M., Barraza, F., Jorquera, H. and Schauer, J. J.: Chemical speciation and source apportionment of fine particulate
1019 matter in Santiago, Chile, 2013, *Sci. Total Environ.*, 512–513, 133–142, <https://doi.org/10.1016/j.scitotenv.2015.01.006>, 2015.
- 1020 Wadinga Fomba, K., Deabji, N., El Islam Barcha, S., Ouchen, I., Mehdi Elbaramoussi, E., Cherkaoui El Moursli, R., Harnafi,
1021 M., El Hajjaji, S., Mellouki, A. and Herrmann, H.: Application of TXRF in monitoring trace metals in particulate matter and
1022 cloud water, *Atmos. Meas. Tech.*, 13(9), 4773–4790, <https://doi.org/10.5194/amt-13-4773-2020>, 2020.

- 1023 Wagner, R., Jähn, M. and Schepanski, K.: Wildfires as a source of airborne mineral dust - Revisiting a conceptual model using
1024 large-eddy simulation (LES), *Atmos. Chem. Phys.*, 18(16), 11863–11884, <https://doi.org/10.5194/acp-18-11863-2018>, 2018.
- 1025 Wang, L., Xin, J., Li, X. and Wang, Y.: The variability of biomass burning and its influence on regional aerosol properties
1026 during the wheat harvest season in North China, *Atmos. Res.*, 157, 153–163, <https://doi.org/10.1016/j.atmosres.2015.01.009>,
1027 2015.
- 1028 Wang, Y., Yang, F., Li, X., Tian, M. and Hopke, P. K.: On the source contribution to Beijing PM_{2.5} concentrations, , 134, 84–
1029 95, <https://doi.org/10.1016/j.atmosenv.2016.03.047>, 2016.
- 1030 Van Wees, D. and Van Der Werf, G. R.: Modelling biomass burning emissions and the effect of spatial resolution: A case
1031 study for Africa based on the Global Fire Emissions Database (GFED), *Geosci. Model Dev.*, 12(11), 4681–4703,
1032 <https://doi.org/10.5194/gmd-12-4681-2019>, 2019.
- 1033 WHO Regional Office for Europe: Air quality guidelines for Europe, pp. 457–465, World Health Organization, Copenhagen,
1034 Denmark, <https://doi.org/10.1525/9780520948068-070>, , 2020.
- 1035 World Health Organization: Review of evidence on health aspects of air pollution - REVIHAAP Project.
1036 [http://www.euro.who.int/pubrequest%0Ahttp://www.euro.who.int/__data/assets/pdf_file/0004/193108/REVIHAAP-Final-](http://www.euro.who.int/pubrequest%0Ahttp://www.euro.who.int/__data/assets/pdf_file/0004/193108/REVIHAAP-Final-technical-report-final-version.pdf)
1037 [technical-report-final-version.pdf](http://www.euro.who.int/pubrequest%0Ahttp://www.euro.who.int/__data/assets/pdf_file/0004/193108/REVIHAAP-Final-technical-report-final-version.pdf), 2013.
- 1038 World Health Organization: WHO global air quality guidelines: particulate matter (PM_{2.5} and PM₁₀), ozone, nitrogen dioxide,
1039 sulfur dioxide and carbon monoxide, World Health Organization. <https://www.who.int/publications/i/item/9789240034228>,
1040 last access: 22 February 2022, 2021.
- 1041 Wu, C. and Zhen Yu, J.: Evaluation of linear regression techniques for atmospheric applications: The importance of appropriate
1042 weighting, *Atmos. Meas. Tech.*, 11(2), 1233–1250, <https://doi.org/10.5194/amt-11-1233-2018>, 2018.
- 1043 Yadav, I. C. and Devi, N. L.: Biomass burning, regional air quality, and climate change, *Encycl. Environ. Heal.*, (April), 386–
1044 391, <https://doi.org/10.1016/B978-0-12-409548-9.11022-X>, 2019.
- 1045 Yadav, S., Tandon, A. and Attri, A. K.: Monthly and seasonal variations in aerosol associated n-alkane profiles in relation to
1046 meteorological parameters in New Delhi, India, *Aerosol Air Qual. Res.*, 13(1), 287–300,
1047 <https://doi.org/10.4209/aaqr.2012.01.0004>, 2013.
- 1048 Yan, J., Wang, L., Fu, P. P. and Yu, H.: Photomutagenicity of 16 polycyclic aromatic hydrocarbons from the US EPA priority
1049 pollutant list, *Mutat. Res. - Genet. Toxicol. Environ. Mutagen.*, 557(1), 99–108,
1050 <https://doi.org/10.1016/j.mrgentox.2003.10.004>, 2004.
- 1051 Yunker, M. B., Macdonald, R. W., Vingarzan, R., Mitchell, H., Goyette, D. and Sylvestre, S.: PAHs in the Fraser River basin:
1052 a critical appraisal of PAH ratios as indicators of PAH source and composition, *Org. Geochem.*, 33, 489–515,
1053 [https://doi.org/doi.org/10.1016/S0146-6380\(02\)00002-5](https://doi.org/doi.org/10.1016/S0146-6380(02)00002-5), 2002.
- 1054